The Resonant Structure of the Kuiper Belt and the Dynamics of the First Five Trans-Neptunian Objects

A. Morbidelli and F. Thomas

Observatoire de la Côte d'Azur, Nice, France

AND

M. Moons

Département de mathématique FUNDP, Namur, Belgium

By means of simple analytic models and numerical integrations, we explore the resonant structure of the Kuiper belt. We find that the inner order-one mean motion resonances with Neptune are very stable and give phase-protection from close encounters with Neptune. The 2/3 resonance is very complex and stable only at small amplitude of libration. The overlapping secular resonances at 36 and 41 AU give rise to large increases in the eccentricity, and therefore to orbits that are very unstable.

Furthermore, we integrate numerically the motion of the first five Kuiper belt objects, the orbits of which have been recently temporarily determined, and we analyze their orbital evolution with respect to resonances. The three objects 1993SB, 1993SC, and 1993RO are in the 2/3 resonance, and, of these, the first two have a very regular evolution. Conversely, 1993RO is chaotic, and is expelled from the 2/3 resonance, encountering Neptune after 320 Myr. The object 1992QB1 is very regular and outside all resonances. Finally, 1993FW is chaotic, due to the 4/7 resonance and to a secondary secular resonance. The eccentricity, however, is limited below 0.2, so that the body does not encounter Neptune. We stress that, since the orbital elements of these five objects are very uncertain, our results should be considered only as indications of possible dynamical evolutions in the Kuiper belt.   © 1995 Academic Press, Inc.

1. INTRODUCTION

The Kuiper belt is nowadays the most fashionable problem in Solar System science. This is due to the discovery of new objects beyond Neptune.

The name "Kuiper belt" has been given in honor of Kuiper, who conjectured that the Sun might be surrounded by a belt made up of comets and comet-like bodies (Kuiper 1951). However, Kuiper was not the first to discuss the existence of the belt, and an earlier paper by Edgeworth (1949) should be mentioned.

Later on, Fernández (1980) pointed out that the Kuiper belt could be the main source of short periodic comets such as those of the so-called "Jupiter family." This was confirmed by Duncan *et al.* (1988) and Quinn *et al.* (1990), although through an artificial model with increased planetary masses which showed that the population of low-inclination comets can be refilled only by a flat disk of quasi-parabolic objects. The Oort cloud would produce comets with isotropically distributed inclinations.

Several works followed from these first results on the relations between the Kuiper belt and the origin of comets (see Stern 1995a, for a review).

It is now generally accepted that low-inclination comets come from the Kuiper belt, although a recent paper by Zheng *et al.* (1995) rehabilitates the Oort cloud, showing that it also could produce a superabundance of comets on prograde low-inclination orbits.

The problem is to understand how comets are transferred from quasi-circular orbits in the Kuiper belt to planet-crossing orbits with large eccentricity. In the outer part of the belt ($a > 1000$ AU) external perturbations exist such as those due to the passage of stars or molecular clouds (Festou *et al.* 1994, Duncan *et al.* 1987); in the inner part only the perturbations given by the giant planets can produce relevant effects. The new objects which have been recently discovered beyond Neptune belong to the inner part of the belt. Then the question arises whether these objects are in stable or unstable orbits with respect to planetary perturbations. In particular, are they potential future comets or rather stable asteroid-like members of the Solar System?

The investigation of the dynamics in the inner part of the Kuiper belt is quite new, and most of the results have been obtained by pure numerical integrations of test particles. The first work was by Torbett and Smoluchowski

(1990), who integrated a number of fictitious objects during a time-span of 10 Myr and found that most of those with a perihelion distance smaller than 45 AU have a positive Lyapunov exponent (of about 1 Myr).

The papers by Holman and Wisdom (1993) and Levison and Duncan (1993) can be considered as a relevant upgrade of Torbett and Smoluchowski's work. By using fast symplectic integrators, these authors could investigate the dynamical behavior of thousands of test particles over, respectively, 2×10^8 and 10^9 years. Both teams found that the dynamics of orbits with $a < 45$ AU is very complex: there are both regions with stable motion over the entire integration time-span and regions with unstable behavior which leads to Neptune-crossing orbits. Unfortunately, they did not try to explain this structure, so that one has the feeling that the phenomena have not been completely understood yet. Nevertheless, these papers provide a huge amount of information; in particular, Holman and Wisdom report the maximal values of the eccentricity and the inclination for each test particle. These two papers inspired us in doing our present study; we will make reference to them and report their main results in Figs. 4 and 9.

Still among the numerical works, one should mention the recent papers by Levison and Stern (1995), in which an extensive exploration of the stability of orbits in the 2/3 resonance with Neptune is carried out, and by Malhotra (1995a), about capture of Kuiper belt bodies into resonances during the early phases of the Solar System. Moreover, while we were revising this paper, a new preprint by Duncan *et al.* (1995) appeared, which is a relevant extension of the previous Levison and Duncan (1993) numerical explorations. In addition, we received a new preprint by Malhotra (1995b), showing Poincaré sections of the dynamics in mean motion resonances with Neptune, computed in the framework of the planar circular three-body problem.

On the branch of analytical studies, the location of secular resonances (i.e., the resonances among the precession rates of the orbits of Kuiper belt objects and of the giant planets) has been first investigated by Heppenheimer (1979), in the framework of the linear theory, and later improved by Knežević *et al.* (1991). Their main result is that the Kuiper belt is quite empty of secular resonances, in contrast to the asteroid belt.

For mean motion resonances, Message (1958, 1959), Schubart (1964), and Beaugé (1994) investigated the dynamics in the outer ones in the framework of the restricted three-body problem, but they made no attempt to apply their analysis to the real case of the Kuiper belt.

In the present paper we explore the specific resonant structure of the Kuiper belt. Our aim is to understand completely the pictures given by Holman and Wisdom (1993) and by Levison and Duncan (1993) and to be able to foretell the distribution of the objects which will be surely found in great number in the inner Kuiper belt. The study is limited to $a < 100$ AU since, outside, planetary perturbations are negligible.

In Section 2 we compute the location and the amplitude of mean motion resonances and investigate their long-term dynamical effects. In Section 3 we study the dynamical behavior of the secular resonances found in Knežević *et al.* (1991). Non-resonant orbits are discussed in Section 4.

Moreover, we study the dynamical nature of the five trans-neptunian objects whose orbits have been recently temporarily determined, and we locate them with respect to resonances. The objects 1993RO, 1993SB, and 1993SC are discussed in Section 2.2, since they are in the 2/3 resonance with Neptune, like the planet Pluto; conversely, 1992QB1 and 1993FW are discussed in Section 4 since their evolution is not permanently dominated by resonances. We stress, however, that the orbital elements of all Kuiper belt objects are, up to now, not precisely known, so that our integrations show some possible dynamical evolutions within the Kuiper belt, rather than the "real" behavior of the newly discovered bodies. We report in Table I the orbital elements assumed as initial conditions for the integrations.

Resonances are not, a priori, regions of unstable and chaotic dynamics; a specific study must be done in order to determine their dynamical nature. In particular, we will show that some mean motion resonances stabilize the long-term evolution, since they provide the mechanisms of protection from Neptune encounters. It is not astonishing, then, that three of the five objects above are in the 2/3 resonance with Neptune.

In the present study, both analytical and numerical tools are used. By perturbation theory, we compute the width of mean motion resonances and build up models for a global view of the long-term dynamics inside mean motion resonances and secular resonances. In Sections 2, 3, and 4, we discuss the results of our analytical computations and their astronomical implications. The celestial mechanics part of our work is described in Section 5; this section can be skipped by all those who are not interested in the mathematical developments of the theory. Moreover, in addition to the analytical computations, we have performed several numerical integrations of evolution of orbits in the Kuiper belt, taking into account the four giant planets of the Solar System. This has been done in order to check our analytic results and to study the evolution of the orbits of the five trans-neptunian objects. For the numerical simulations we have used the symplectic integrator designed by Levison and Duncan (1994), which is based on the original algorithm by Wisdom and Holman (1991), but is in the public domain. This program is well done, well documented, and very fast and precise. Unfortunately, the version of the program which is in the public domain cannot handle planetary close encounters; how-

TABLE I
Table of Initial Conditions

Object	a (AU)	e	i (°)	ω (°)	Ω (°)	M (°)	Epoch	Source
1992 QB1	43.7638298	0.0682194	2.21151	16.89418	359.41255	346.74074	1993 Aug. 1.0	M.P.C. 22594
1993 FW	43.9084197	0.0405841	7.73665	8.21749	187.91448	353.07070	1994 Feb. 17.0	M.P.C. 23240
1993 RO	39.6956195	0.2046118	3.72341	184.52897	170.30328	358.17942	1994 Sept. 5.0	M.P.E.C. 1994-R06
1993 SB	39.4213949	0.3213859	1.92850	79.01471	354.81023	318.99486	1994 Sept. 5.0	M.P.E.C. 1994-S06
1993 SC	39.4708367	0.1795353	5.16078	319.22139	354.64420	33.90431	1995 Mar. 24.0	M.P.E.C. 1995-C16

ever, it is adequate for the goals of this paper. Indeed, we are interested here in the mechanisms for transporting Kuiper objects to Neptune and not in the further evolution of their orbits, dominated by encounters.

2. MEAN MOTION RESONANCES IN THE KUIPER BELT

The location of mean motion resonances can be very simply computed according to Kepler's third law. It is much more difficult to determine the width of the resonances, and this needs some tools of analytic celestial mechanics. The results are summarized in Fig. 1, which gives the location and width of the main mean motion resonances with Neptune and Uranus on the $a-e$ plane between 30 and 100 AU. The computation has been done in the framework of the circular restricted three-body problem. The masses of the non-resonant planets have been added to that of the Sun. The inclination of the Kuiper belt bodies is assumed to be zero.

The n/m resonances with Neptune are denoted by the label Nn/m; those with Uranus by Un/m. For each resonance, the vertical line traces its location and the diamond-like curves delimit the width. Continuous curves refer to resonances with Neptune, while dashed curves refer to those with Uranus.

The two bold lines denote Neptune-crossing orbits and Uranus-crossing orbits with perihelion distances of 30.11 and 19.22 AU, respectively. The dotted line denotes a perihelion distance equal to 32 AU, where the effects of close encounters with Neptune are observed to become relevant in the numerical integrations.

However, an object at the center of a mean-motion resonance with Neptune is phase-protected from close encounters with the planet. This is the reason the lines denoting mean motion resonances with Neptune are plotted up to the Uranus-crossing limit. Orbits in mean motion resonances with Neptune are not protected from Uranus close encounters. For the same reason, the mean motion resonances with Uranus are only plotted up to the Neptune-crossing limit.

The width of the mean motion resonances with Neptune changes abruptly in correspondence to the Neptune-cross-

ing limit. Indeed, resonant orbits with large amplitudes of libration can enter into collision with the planet. Therefore, the non-encountering condition gives a constraint on the amplitude of libration of resonant orbits, so that the width
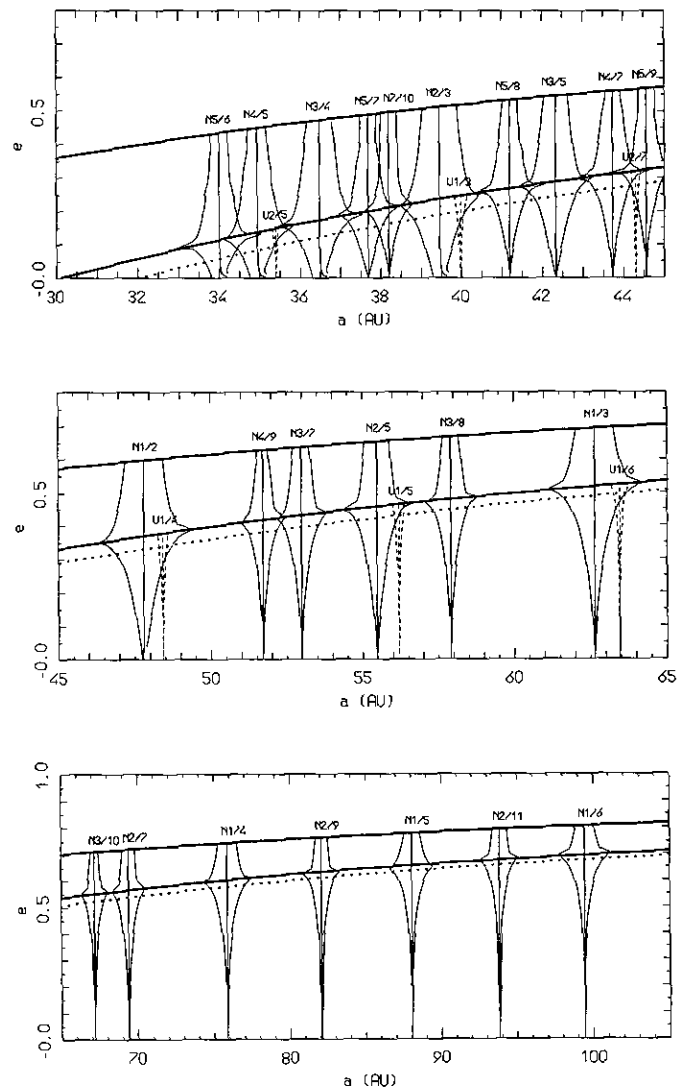

FIG. 1. The location and the width of mean motion resonances with Neptune and Uranus in the Kuiper belt between 30 and 100 AU. See text for description.

of the resonant region which is stable with respect to Neptune encounters shrinks with increasing eccentricity. We will give in Section 5 more details on the computation of the resonant width both above and below the planet-crossing line.

Figure 1 shows the importance that mean motion resonances have in structuring the Kuiper belt. In particular, in the inner part of the Kuiper belt ($a < 45$ AU), there are several resonances with non-negligible width. Among them, the sequence of resonances of order one, i.e., 2/3, 3/4, 4/5, 5/6, converges toward the orbit of Neptune. These resonances overlap only partially, near the Neptune-crossing threshold. The overlap of mean motion resonances usually indicates large scale chaos; in this case this should happen only in a region which is already strongly perturbed due to close Neptune encounters.

Beyond 45 AU, the low-order mean motion resonances are more separated. Moreover, apart from the 1/2, 2/5 and 1/3 resonances, they are very thin so that the volume occupied by them in the small eccentricity part of the diagram is negligible. In short, below 45 AU the Kuiper belt is strongly sculptured by the presence of mean motion resonances, while at $a > 45$ AU it is essentially non-resonant. Apart from these considerations, Fig. 1 does not provide any indication about the stability of the dynamics in mean motion resonances. One has to investigate the effects of Neptune's eccentricity and, especially, of the secular changes of the planetary orbital elements.

2.1. Dynamics in the Inner Order-One Resonances

This section is devoted to resonances 3/4, 4/5, and 5/6 with Neptune which dominate the Kuiper belt at $a < 37$ AU. These resonances are characterized by mostly regular motion at moderate eccentricity. As an example, we show in Fig. 2 the result of the numerical integration of a fictitious body in the 5/6 resonance with initial eccentricity $e = 0.1$, perturbed by the four giant planets. The four panels show the evolution over 10 Myr of the semimajor axis, of the critical angle of the resonance $\sigma = -5\lambda_N + 6\lambda - \varpi$ (λ and λ_N are the mean longitudes of the body and of Neptune, respectively, and ϖ denotes the body's longitude of perihelion), of the eccentricity, and of the inclination. There is very regular behavior of the orbital elements, which change quasi-periodically with time; such a regularity suggests that the orbit must be stable over a time scale much longer than 10 Myr. We stress that the eccentricity is so large that the perihelion distance becomes smaller than 29.8 AU. Nevertheless, there are never close encounters with Neptune, since the body is deeply inside the mean motion resonance, the critical angle σ librating with small amplitude ($\pm 30°$) around the stable resonant value $\sigma = 180°$. The eccentricity oscillates between 0.09 and 0.12; we have checked that this oscillation is coupled to the circulation of
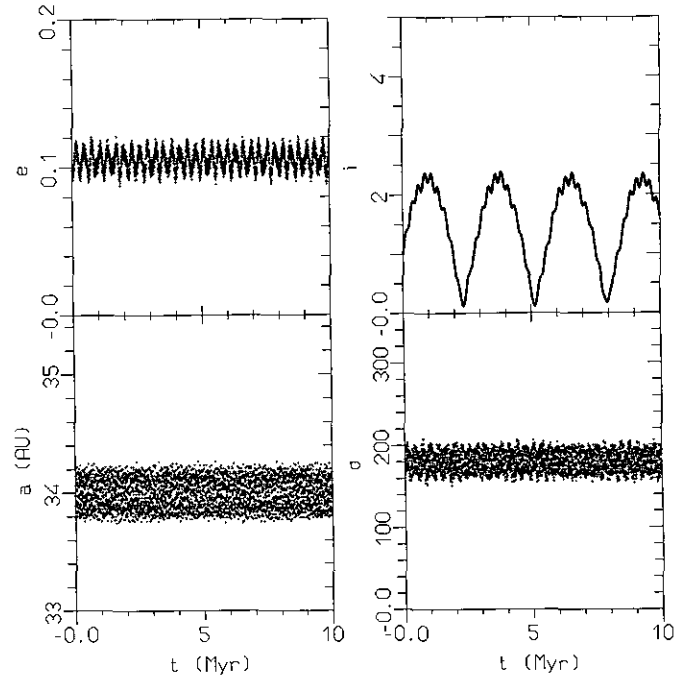

FIG. 2. The time evolution of the heliocentric orbital elements of a fictitious orbit in the 5/6 resonance with Neptune. The critical angle of the 5/6 resonance is $\sigma = -5\lambda_N + 6\lambda - \varpi$.

$\varpi - \varpi_N$, ϖ_N being the longitude of perihelion of Neptune. Orbits with initially smaller eccentricity are characterized by faster oscillations of e. The inclination changes from 0 to 2.5° with respect to the invariable plane of the outer Solar System; its oscillation is coupled with the circulation of $\Omega - \Omega_N$, which are the longitudes of the nodes of the body and of Neptune, respectively.

We have found numerically the same kind of behavior as in Fig. 2 for orbits in the 4/5 and 3/4 resonances. We have therefore elaborated on a theoretical model to explain such a generalized stability. The main point is that in a mean motion resonance of order one, such as the 5/6, 4/5, and 3/4 resonances, the longitude of perihelion ϖ must circulate clockwise (i.e., $\dot\varpi < 0$): the opposite direction with respect to planetary perihelia; this circulation is very fast if the eccentricity has small to moderate values (see Section 5). Therefore, no secular resonance can occur between the motions of the perihelia of the body and of the perturbing planets, at small eccentricity. As a consequence, the eccentricity oscillates fast and with small amplitude. In order to emphasize this fact, we plot in Fig. 3 the secular evolution of the eccentricity with respect to the circulation of $\varpi - \varpi_N$. This figure has been computed under the assumption that only Neptune is present with eccentricity $e_N = 0.0147$. In addition, the σ-libration in the 5/6 resonance is assumed to be small, and the inclination i is assumed to be 0. As is easily seen, the phase space is foliated
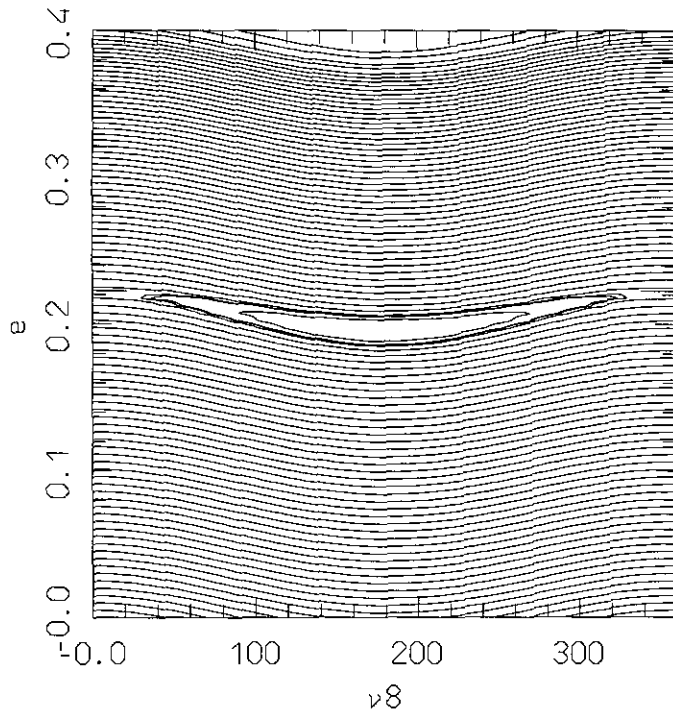
FIG. 3. The secular evolution of the eccentricity as a function of $\nu_8 \equiv \varpi - \varpi_N$ for orbits deeply inside the 5/6 mean motion resonance with Neptune. The phase space is foliated with slightly distorted invariant tori, apart from the region around $e = 0.2$, where $\varpi - \varpi_N$ librates.

with slightly deformed invariant tori at small eccentricity ($e < 0.2$), where the fast rotation of $\varpi - \varpi_N$ forces only small amplitude oscillations of the eccentricity. At $e = 0.2$, ϖ and ϖ_N are in resonance and $\varpi - \varpi_N$ librates. The same is true in the 4/5 and 3/4 resonances, where the resonance corresponding to the libration of $\varpi - \varpi_N$ moves to larger eccentricity.

All our theoretical and numerical computations assess the great regularity of the mean motion resonances of order one in the inner Kuiper belt; nevertheless, some chaotic regions can always be found, for example, for orbits with large amplitude of σ-libration or close to some possible secondary resonance between the period of libration of σ and the period of circulation of $\varpi - \varpi_N$. The dominant dynamical character of these mean motion resonances is regularity; however, the existence of some chaotic and unstable resonant orbits cannot be excluded.

Coming now to the numerical results by Levison and Duncan (1993), we reproduce in Fig. 4 their diagram concerning the stability times of orbits with initial eccentricity $e = 0.1$ in the Kuiper belt. Evident "stability peaks" appear between 34 and 40 AU. In light of our results, the peaks at $a = 35$ AU and $a = 36.5$ AU are very probably associated with the 4/5 and 3/4 resonances. The small peak of stability up to less than 10 Myr at $a = 34$ AU is evidently associated

with the 5/6 resonance. Why is the stability time so short? The example reported in Fig. 2 is stable up to at least 10 Myr. We guess that this is simply an artifact of the method that Levison and Duncan used to compute the "stability times." Indeed, they wrote that "each particle was integrated for 1 Gyr unless it was removed because it either crossed Neptune's orbit or suffered a close approach to Neptune." However, particles in the 5/6 resonance can cross the orbit of Neptune safely, without running the risk of any close encounter with the planet. In this case, therefore, we suspect that the real stability time has been largely underestimated by Levison and Duncan.

From Levison and Duncan's results (Fig. 4), two additional thinner stability peaks appear at $a = 37.7$ AU and $a = 38.3$ AU, which are probably connected with the 5/7 and 7/10 mean motion resonances with Neptune. Our numerical tests confirm that the 5/7 resonance has very regular orbits. A further double stability peak is present at 39–39.5 AU; this is probably associated with the 2/3 resonance. The dynamics in the 2/3 resonance is much more complicated, so that a full section must be devoted to the discussion of this case.

2.2. Dynamics in the 2/3 Resonance

The long-term dynamical evolution in the 2/3 resonance is complex since, inside of the resonance itself, some secular resonances are present.

In the asteroid belt, secular resonances can be found inside many mean motion commensurabilities. In particular, the overlap of secular resonances inside mean motion commensurabilities is the basis of the origin of most of the Kirkwood gaps (Wisdom 1985, Morbidelli and Moons 1993, Moons and Morbidelli 1995).
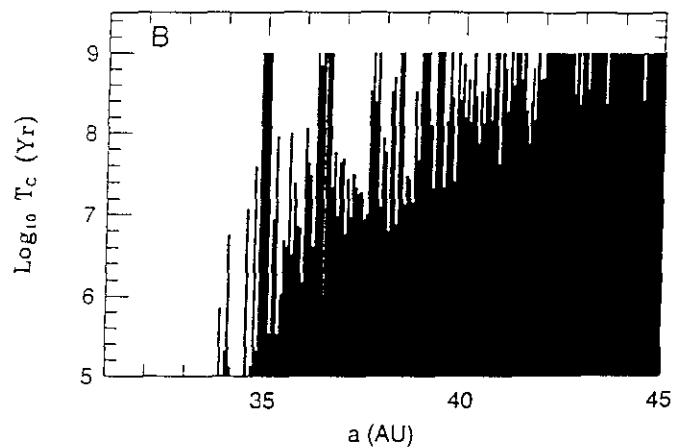

FIG. 4. From Levison and Duncan (1993): the stability times of orbits with initial eccentricity $e = 0.1$, as a function of the semimajor axis. See text for comments.

The order-one resonances analyzed in the previous section are characterized by a very stable dynamics since secular resonances are not present at small eccentricity.

In the case of the 2/3 resonance, conversely, the Kozai resonance and the ν_{18} resonance can be found, if the perturbation of the four giant planets is taken into account.

The Kozai resonance concerns the libration of the argument of perihelion ω. Everybody knows, since the numerical integration by Williams and Benson (1971), that the argument of perihelion of Pluto librates. Nacozy and Diehl (1974, 1978) and Kozai (1985) computed analytically the evolution of its eccentricity and inclination coupled with the ω-libration. Here, we have computed the location and the width of the Kozai resonance for orbits which are deeply inside the 2/3 commensurability, i.e., such that the critical argument $\sigma = -2\lambda_N + 3\lambda - \varpi$ librates with small amplitude around the stable resonant value $\sigma = 180°$.

Figure 5 gives the results on the e–i plane; the inclination is measured with respect to the invariable plane. The value of the semimajor axis is that of the exact 2/3 resonance. The present position of Pluto is marked by a circle.
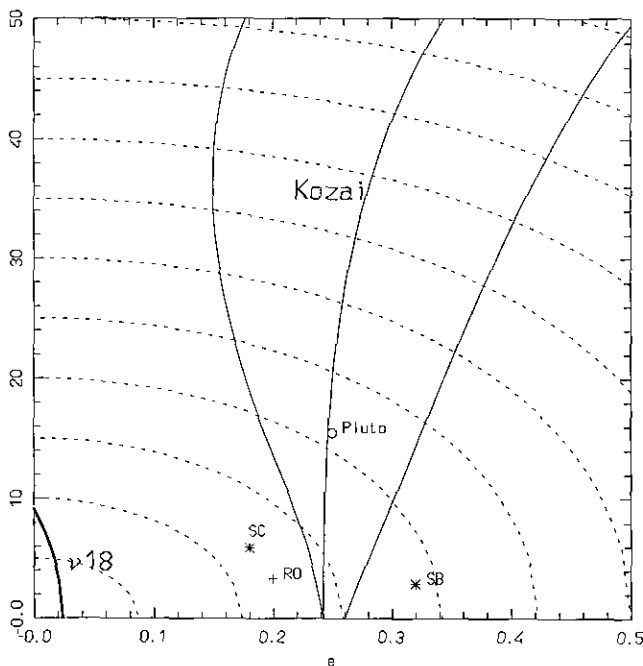

FIG. 5. Phase space of the secular dynamics in the 2/3 resonance with Neptune. The picture is computed for orbits with small amplitude of σ-libration. It shows the Kozai resonance (the center line denoting its location and the side lines its width) and the ν_{18} resonance (the bold line denoting its location). The dashed curves denote the levels of the z-component of the angular momentum. The two asterisks mark the present position of 1993SC and 1993SB, the circle marks the present position of Pluto, and the cross marks the present position of 1993RO. However, 1993RO librates with large amplitude, so that its position with respect to the Kozai resonance must be considered only as qualitative. The inclination is measured with respect to the invariable plane.

The effect of the Kozai resonance is to force the oscillations of e and i; the eccentricity and the inclination are coupled and must evolve along one of the dashed lines plotted in Figure 5, which are the level curves of the z-component H of the angular momentum.

The ν_{18} secular resonance occurs when the precession rate s of the body's nodal longitude Ω is equal to the average precession frequency s_8 of Neptune's node Ω_N. The effect of the ν_{18} resonance is to pump up the inclination of the resonant body. The location of the ν_{18} resonance inside the 2/3 commensurability is indicated by a bold line in Fig. 5. The ν_{18} resonance is located at very small eccentricity and is well separated from the Kozai resonance. We have numerical evidence, however, that this separation becomes narrower with increasing amplitude of σ-libration inside the 2/3 commensurability; indeed, the ν_{18} resonance moves to larger eccentricity and the Kozai resonance moves to smaller eccentricity. This can explain why, in their recent paper on the origin of Pluto, Levison and Stern (1995) found numerical evidence that strong instability occurs when the amplitude of libration of σ is large.

In Fig. 5 we mark by asterisks the presently assumed position of the Kuiper belt objects 1993SC and 1993SB. These two objects are in the 2/3 resonance and their amplitude of σ-libration is small, as we have checked in a 500-Myr integration (Figs. 6 and 7, respectively). Therefore, for these two bodies, Fig. 5 is quite accurate, and shows that 1993SC and 1993SB are protected from both the Kozai resonance and the ν_{18} resonance, provided their orbital elements are confirmed. As a consequence, a very regular behavior is expected. As seen in Figs. 6 and 7, the evolution of their semimajor axis, eccentricity, and inclination looks smooth and quasi-periodic. In order to check the position of the two objects with respect to the ν_{18} and to the Kozai resonances, the first 30 Myr of the evolution of the resonant critical angles are magnified. The critical angle of the ν_{18} resonance, i.e., $\Omega - g_8 t \simeq \Omega - \Omega_N$ circulates with a period of about 4 Myr in both cases, which implies that the resonance is far away. The critical angle ω of the Kozai resonance circulates with negative derivative in the case of 1993SC and with positive derivative in the case of 1993SB; this proves that the former is on the left-hand side of the Kozai resonance while the latter is on the right-hand side. This confirms the theoretical result shown in Fig. 5.

Still in Fig. 5, a cross denotes the assumed "position" of 1993RO, which is also in 2/3 resonance with Neptune. However, from our numerical integration (Fig. 8), the amplitude of σ-libration of 1993RO is quite large while the location of the Kozai resonance in Fig. 5 has been computed in the limit of small σ-libration. Figure 5, then, must be considered only as qualitative in this case; in particular, the Kozai resonance should be somewhat closer to the object than Fig. 5 shows. The long-term evolution of 1993RO obtained by numerical integration is strongly cha-
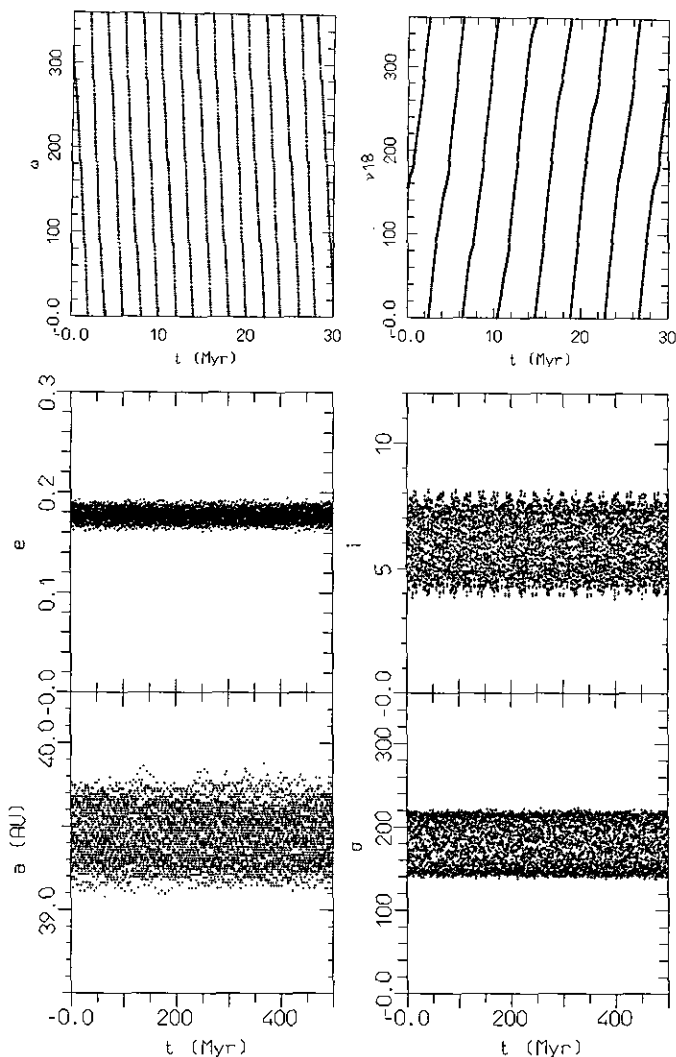
The fact that in this integration 1993RO is eliminated in 320 Myr implies nothing for its real evolution. Since the orbit is strongly chaotic, the integration is not predictive. The real object could evolve in a different way and on different time scales. Moreover, it is possible that future improvements of its orbital elements, which are still very uncertain, will put 1993RO in the stable region of the 2/3 resonance. As a matter of fact, in the most recent preprint by Duncan *et al.* (1995) new orbital elements are taken into account (the eccentricity being decreased to 0.12), which make 1993RO stable over 1 Gyr.

In conclusion, the 2/3 resonance with Neptune has a very complex dynamics, since both regular and chaotic orbits coexist. The larger the amplitude of σ-libration, the more irregular the dynamics becomes (see also Levison and Stern 1995, Duncan *et al.* 1995). Indeed, if the
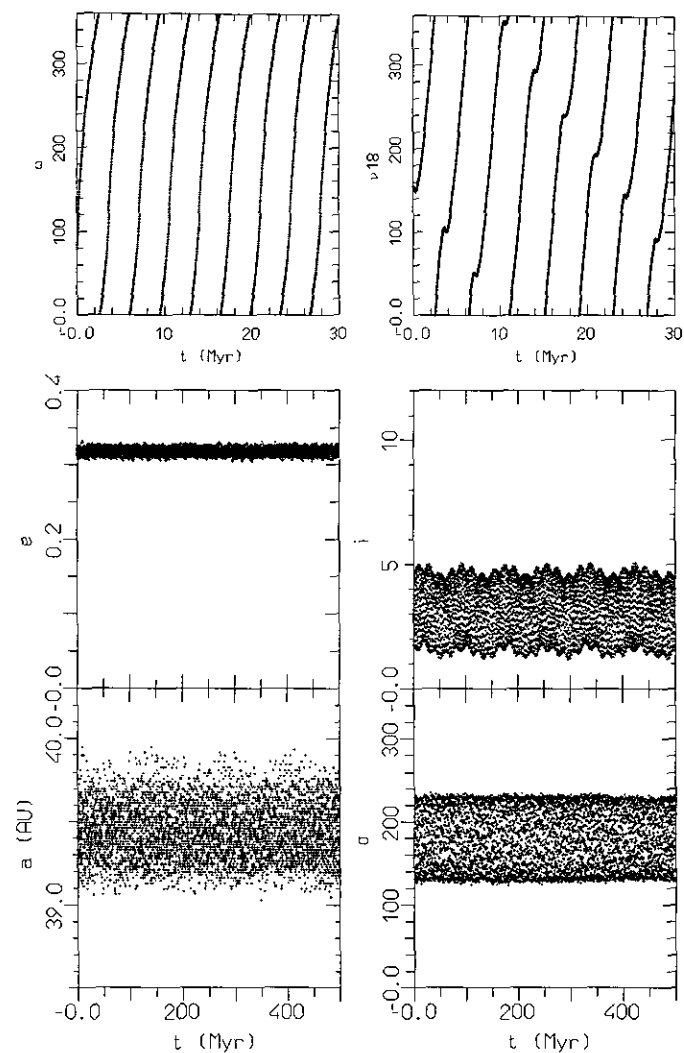

FIG. 6. The time evolution over 500 Myr of the heliocentric orbital elements of 1993SC. Initial conditions are those reported in MPEC1995-C17. The two top pictures show the magnification over 30 Myr of the motion of the argument of perihelion ω and of $\nu_{18} \equiv \Omega - \Omega_N$. Moreover, the critical angle σ of the 2/3 resonance is defined as $-2\lambda_N + 3\lambda - \varpi$. See text for comments.

otic. The behavior of the eccentricity and of the inclination is very irregular. This is due precisely to the Kozai resonance. Indeed, the object is temporarily trapped by the Kozai resonance as the evolution of the argument of perihelion shows: there are temporary librations around $\omega =$ 0°, 180°, or 90°. The amplitude of σ-libration increases along the chaotic evolution of the orbit. When σ librates with large amplitude, the ν_{18} resonance is crossed, causing large jumps in the inclination. From 200 Myr, the object is temporarily ejected from the resonance (σ circulates). At these times, 1993RO is no longer protected from close encounters with Neptune. At 320 Myr a strong close encounter occurs, so that the integration is stopped.

FIG. 7. The same as Fig. 6 for 1993SB. Initial conditions are taken from MPEC1994-S06.

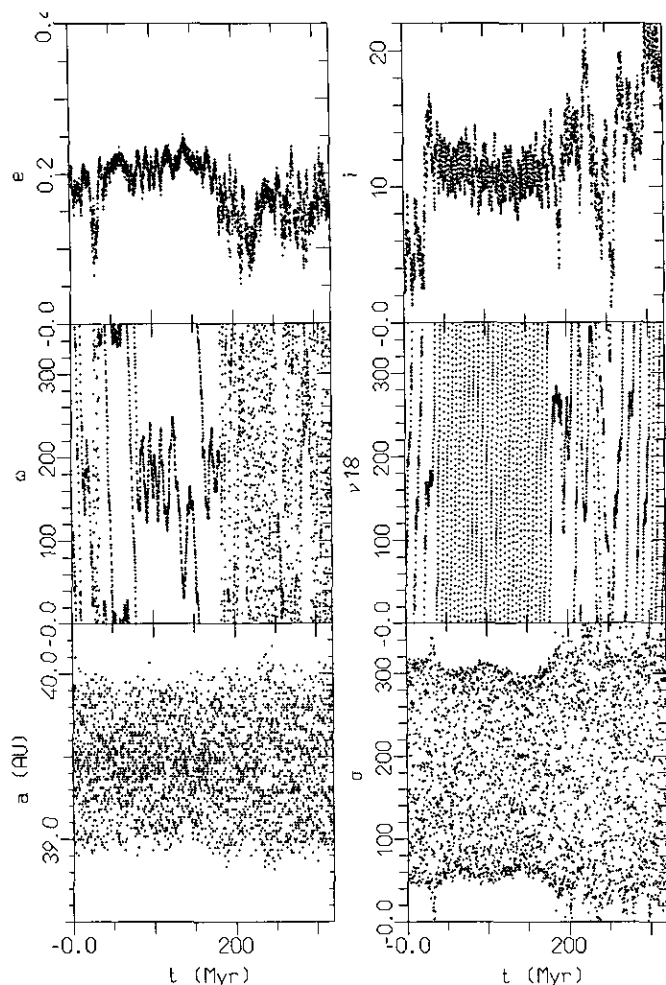FIG. 8. The time evolution over 320 Myr of the heliocentric elements of 1993RO. Initial conditions are taken from MPEC1994-R06. Again, $\nu_{18} \cong \Omega - \Omega_N$ and $\sigma = -2\lambda_N + 3\lambda - \varpi$. The object is ejected by a close encounter with Neptune at 320 Myr. See text for comments.

amplitude of σ-libration is very large, the ν_{18} resonance and the Kozai resonance join together, and their interaction gives rise to large scale chaos, as seen in the case of 1993RO.

As a confirmation of the coexistence of both regular and chaotic motion within the 2/3 resonance, note that Levison and Duncan (1993) found a double peak of stability up to 1 Gyr, separated by an instability gap around 39.5 AU (Fig. 4); this is possibly due to the fact that some of the 2/3 resonant orbits, probably those with large amplitude of σ-libration, escape (see also Duncan et al. 1995). Moreover, Holman and Wisdom (1993) found, in correspondence to the 2/3 resonance, orbits whose eccentricities become larger than 0.2 as well as orbits whose maximal eccentricities are bounded below 0.1 (their picture is reproduced in Fig. 9).

2.3. Dynamics in the Outer Mean Motion Resonances

The outer mean motion resonances ($a > 45$ AU) are much less important than the inner ones for the structure of the Kuiper belt. On one hand, since Neptune is far away, these resonances do not play a fundamental role in protection from close encounters with the planet. On the other hand, they do not force large changes in the eccentricity of resonant bodies, so that they cannot be considered as active transport channels from the Kuiper belt to the planetary region.

The 1/2 resonance with Neptune has the particularity that the critical angle of the resonance $\sigma = -\lambda_N + 2\lambda - \varpi$ can librate not only around $\sigma = 180°$, but also around two symmetric values $\sigma = 180° \pm \Delta\sigma$, the value of $\Delta\sigma$ depending on the eccentricity. In the framework of the planar circular three-body problem, the typical resonant phase space is that shown in Fig. 10 with respect to the coordinates $k = e \cos \sigma$ and $h = e \sin \sigma$. Two islands of libration appear, which are symmetric with respect to the x-axis, and which are included in a large island of libration around $\sigma = 180°$. The equilibrium at $\sigma = 180°$ is unstable. This result for the 1/2 resonance is not new, and we refer to the paper by Schubart (1964) and to the recent one by Beaugé (1994) for further details. We have found in our study that all resonances of the kind $1/n$ have axisymmetric islands of libration. Note that we have always considered the largest island of libration for the determination of the widths of the $1/n$ resonances in Fig. 1.

The presence of two axisymmetric islands inside the large island of libration and the existence of a separatrix surrounding them give rise to some local chaos inside these mean motion resonances. As an example, Fig. 11 shows the evolution of σ for a fictitious body in the 1/2 resonance: the orbit is temporarily captured into one of the two axisymmetric islands; thus, the behavior of the eccentricity is somewhat irregular.

Orbits with initially very large amplitude of σ-libration in the large island show some chaotic behavior as well, with temporary expulsion from the 1/2 resonance and circulation of σ.

Apart from these cases of "local chaotic behavior," we have found no numerical evidence of wildly unstable motion nor of large scale chaos in the 1/2, 2/5, or 1/3 resonances with Neptune, for moderate eccentricity ($e < 0.3$)— nothing similar to what happens in the 3/1 and in the 5/2 resonances with Jupiter in the asteroid belt. The qualitative reason for this is that the planetary perturbations in this outer part of the belt are weak, so that the longitude of perihelion ϖ and the longitude of node Ω move very slowly, much more slowly than those of the planets. Therefore, no low order secular resonance can occur inside these mean motion commensurabilities.
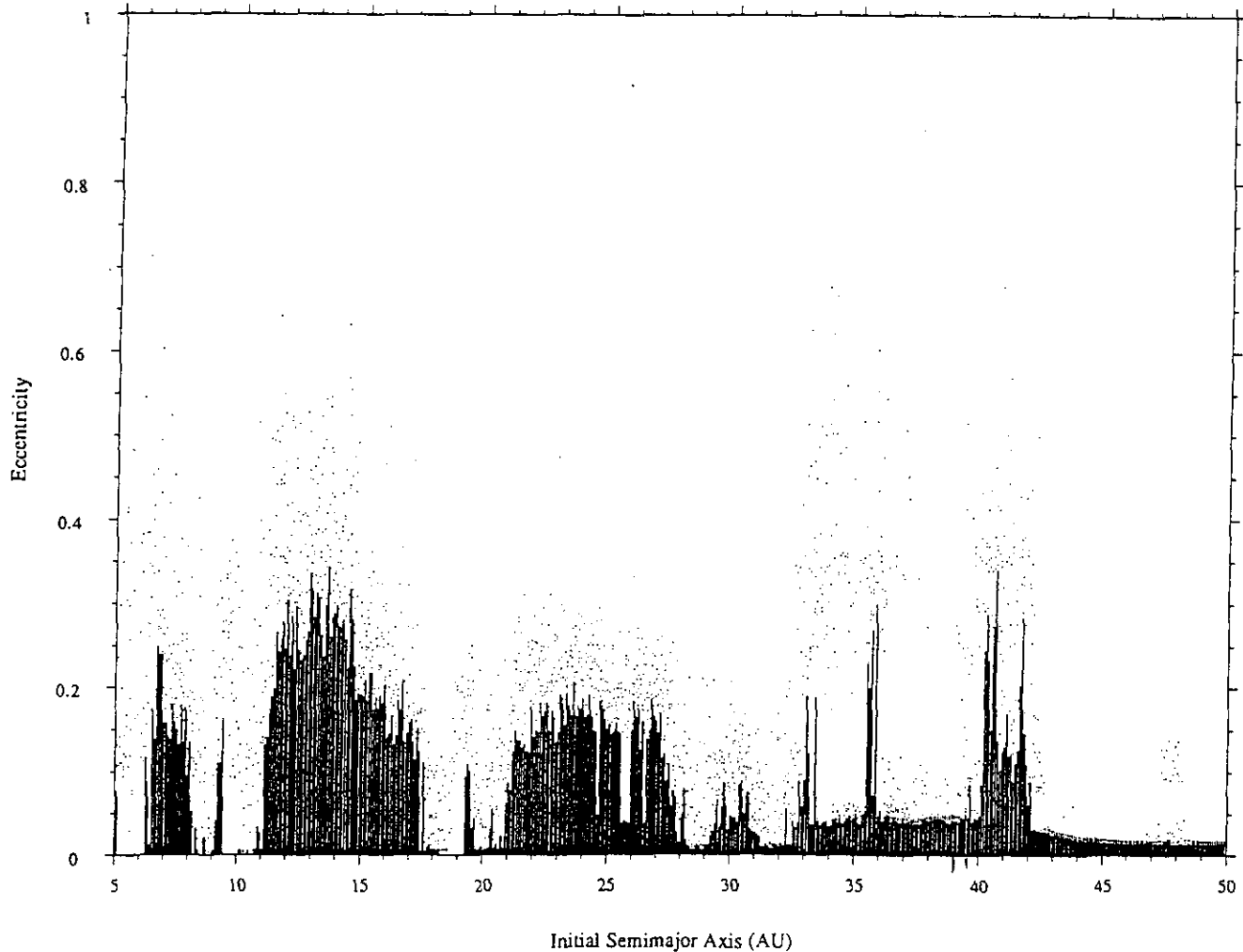
This can be seen also in Holman and Wisdom's paper

FIG. 9. From Holman and Wisdom (1993): the maximal eccentricity of test orbits as a function of the semimajor axis. For each semimajor axis six test particles were started at different longitudes. The points denote the maximal eccentricity attained by each test particle during the course of the integration. The vertical bars mark the minimum of the six values.

(1993) (see Fig. 9), where the maximal eccentricity of initially circular orbits in the 1/2 resonance is found to be less than 0.15.

3. SECULAR RESONANCES

Secular resonances can be found *outside* mean motion commensurabilities, and this section is devoted precisely to exploring the dynamical behavior in these cases.

For the location of secular resonances, Knežević *et al.* (1991) pointed out that in the range 40–42 AU the ν_8, the ν_{18}, and the ν_{17} secular resonances can be found and the convergence of the ν_7, ν_8, and ν_{17} resonances at 36 AU, at the limit of the region covered by their investigation. The ν_8 secular resonance occurs when the precession rate g of the body's longitude of perihelion ϖ is equal to the

precession frequency g_8 of Neptune's longitude of perihelion ϖ_N; the ν_7 resonance occurs when g is equal to the precession frequency g_7 related to Uranus' perihelion ϖ_U; the ν_{17} resonance is given by $s = s_7$, s and s_7 being the nodal precession frequencies of the body Ω and of Uranus Ω_U, respectively; the ν_{18} resonance is the corotation with the node of Neptune (Section 2.2).

Holman and Wisdom (1993) found large increases in both the eccentricity and the inclination between 40 and 42 AU and a large increase in the eccentricity between 35 and 36 AU (Fig. 9).

We have elaborated two simple models, taking into account the perturbations of the four giant planets, to show the global portrait of the secular dynamics in the ν_8 and ν_{18} resonances at $a = 41.5$ AU and $a = 40$ AU, respectively (Fig. 12). The ν_8 model shows that the eccentricity is
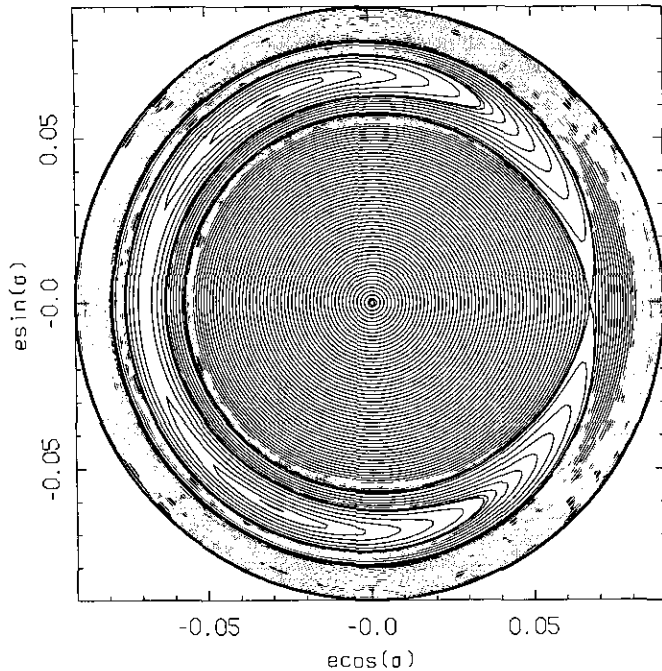
FIG. 10. The phase space of the 1/2 mean motion resonance with Neptune in the framework of the planar circular problem. Note the two axisymmetric islands of libration. The critical angle of the resonance is $\sigma = -\lambda_N + 2\lambda - \varpi$. The value of $N - S_z$ is equal to -2.08, measuring a in AU (see Section 5).

pumped up from 0 to 0.2 by the libration of the critical angle of the resonance $\varpi - g_8 t \sim \varpi - \varpi_N$. At $e = 0.2$, close encounters with Neptune can occur, since the secular resonance does not provide any mechanism of protection from close approaches. The ν_{18} model shows that the inclination is pumped up from $0°$ to about $10°$ by the libration of the critical angle of the resonance $\Omega - s_8 t \sim \Omega - \Omega_N$. However, these models are computed in the approximation that each resonance is isolated; in particular, in the ν_8 model the inclination is assumed to be $0°$, and in the ν_{18} model the eccentricity is assumed to be 0. This is evidently a very crude approximation. Indeed, the two secular resonances coexist in the region 40–42 AU, and their interaction cannot be neglected. The interaction of resonances gives rise to large scale chaos, and predictive analytic models of the dynamical behavior of resonant orbits can no longer be developed. Moreover, the secondary secular resonance $\nu_8 + \nu_{18}$, i.e., the one where $g + s = g_8 + s_8$, comes into play, complicating the dynamical picture even more. This three-resonance interaction is something which is quite new in celestial mechanics: in the asteroid belt, secular resonances are well separated, and each of them can be studied by predictive analytic models (Morbidelli 1993). The only exception is the intersection of the ν_5 and ν_{16} resonances at large inclination.

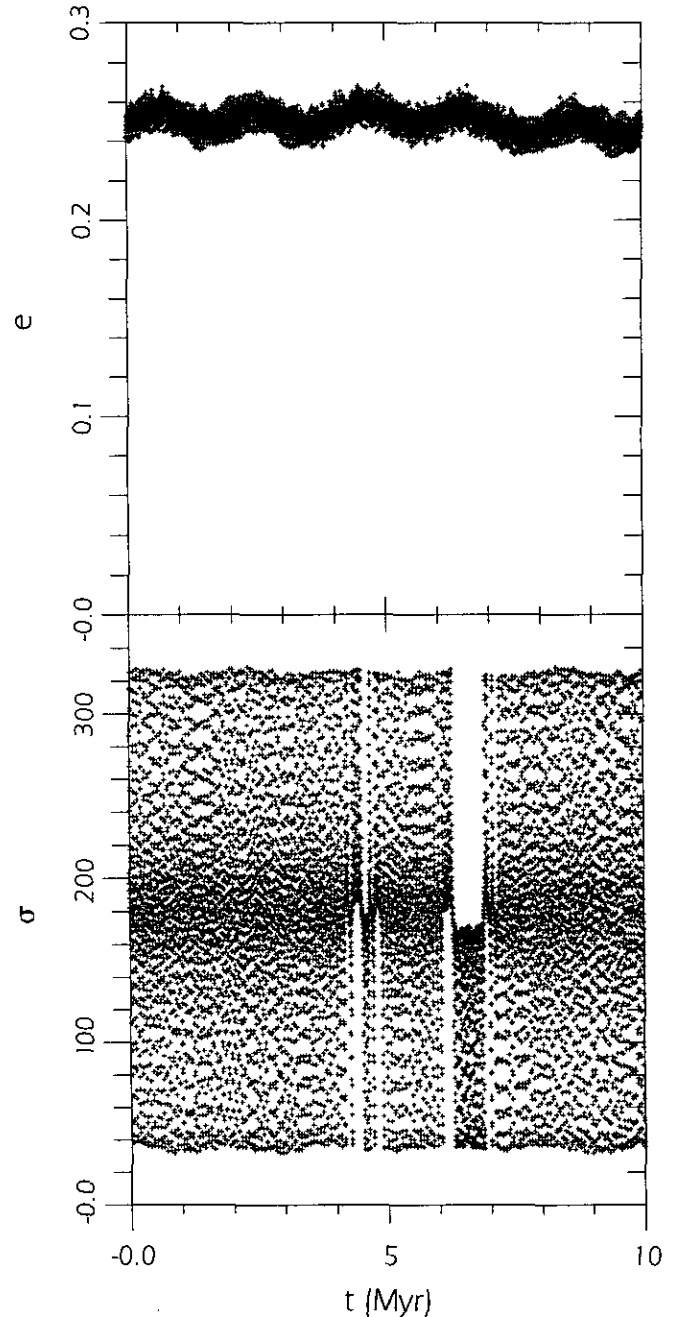We have performed some numerical integrations of test

FIG. 11. The time evolution of the heliocentric elements of a fictitious particle in the 1/2 resonance with Neptune. The critical angle $\sigma = -\lambda_N + 2\lambda - \varpi$ is temporarily captured in axisymmetric libration. See text for details.

objects in the region 40–42 AU, over a 40 Myr timespan. All confirm the great chaotic character of this region, with large increases in both the eccentricity and the inclination and short stability time as found by Holman and Wisdom (1993) and Levison and Duncan (1993). Close encounters with Neptune occur very rapidly. As an example, Fig. 13
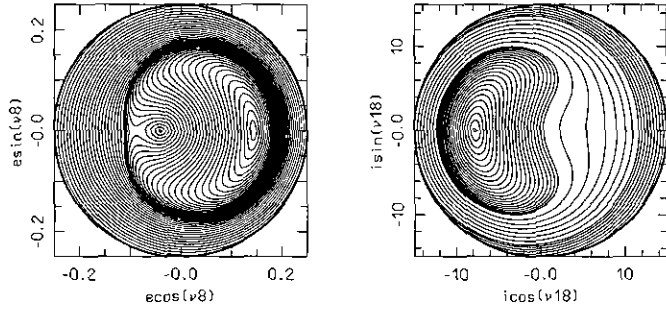
FIG. 12. (Left) the phase space of the ν_8 resonance, computed at $a = 41.5$ AU and $i = 0$. The label ν_8 denotes the critical angle of the resonance $\varpi - \varpi_N$. (Right) the phase space of the ν_{18} resonance, computed at $a = 40$ AU and $e = 0$. The label ν_{18} denotes the critical angle of the resonance $\Omega - \Omega_N$.

FIG. 14. Time evolution of a fictitious object in the 36 AU region. The evolution is chaotic due to the overlapping ν_8 and ν_7 secular resonances. Here ν_8 denotes $\varpi - \varpi_N$ and ν_7 denotes $\varpi - \varpi_U$.
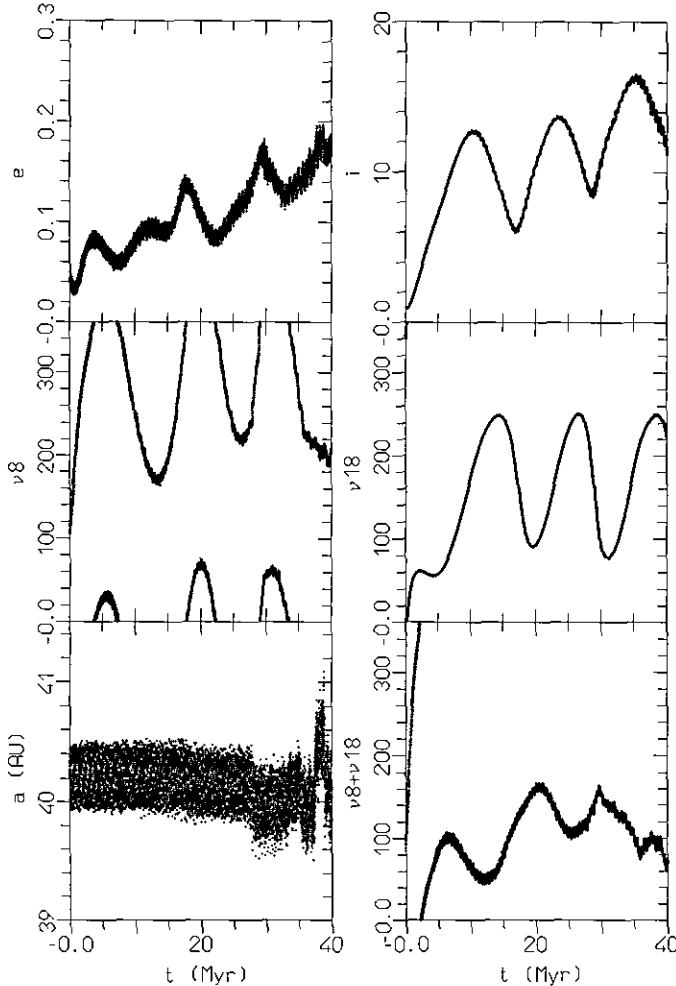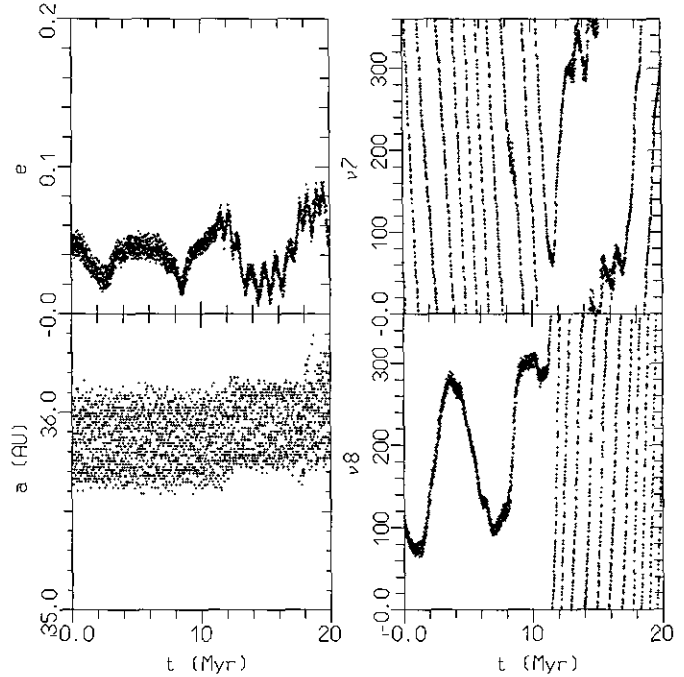

FIG. 13. Time evolution of a fictitious object in the 40–41 AU region. The orbit is strongly chaotic due to the copresence of several secular resonances. Here ν_8 denotes $\varpi - \varpi_N$, ν_{18} denotes $\Omega - \Omega_N$, and $\nu_8 + \nu_{18}$ denotes $\varpi + \Omega - \varpi_N - \Omega_N$.

shows the evolution of the eccentricity, of the inclination, of the semimajor axis, and of the critical angles of the secular resonances ν_8, ν_{18}, and $\nu_8 + \nu_{18}$ for a test particle with initial semimajor axis $a = 40.4$ AU. The critical angle of the ν_8 resonance librates around $0°$ and the critical angle of the ν_{18} resonance librates around $180°$, as predicted by the models in Fig. 12. However, due to the strong resonance interactions, the dynamical evolution is not regular, and the critical angles change their libration amplitude and temporarily circulate. As a consequence, the eccentricity and the inclination are not quasi-periodic with time. At the end of the integration span, strong close encounters with Neptune occur, as one can deduce from the jumps of the semimajor axis.

In the region at 35–36 AU, the interactions between the ν_8 and ν_7 secular resonances give rise to large scale chaos and prevent the definition of a predictive analytic model. Figure 14 shows the evolution of a test particle with initial $a = 36$ AU. The behavior of the eccentricity is very irregular. The critical angle of the ν_8 resonance librates at the beginning of the integration, which means that the body is in the ν_8 resonance. Then it circulates very quickly, while the critical angle of the ν_7 resonance slows and eventually librates temporarily, which shows capture into the ν_7 resonance. The overlap of these two secular resonances is responsible for chaos. At the end of the 20-Myr integration timespan a very strong encounter with Neptune occurs.

4. NON-RESONANT ORBITS AND THE EVOLUTION OF 1992QB1 AND 1993FW

This section deals with orbits which are not in the secular resonances or in the unstable parts of mean motion commensurabilities discussed above. In these cases the eccentricity does not increase much, as can be checked from Holman and Wisdom's numerical result (Fig. 9). This is due to the absence of resonant perturbation effects.

In the inner part of the Kuiper belt, however, non-resonant orbits are not protected from close encounters with Neptune, so that they turn out to be strongly unstable. In Levison and Duncan's result (Fig. 4) one notes that, apart from the resonant stability peaks, the stability time increases from 10^5 years at 34–35 AU to 10^9 years at 42 AU for orbits with initial eccentricity $e = 0.1$. This is due to the fact that, the larger the semimajor axis, the larger is the perihelion distance; thus, the typical lifetime before a strong close encounter with Neptune increases. Similarly, if the initial eccentricity is 0.01, the stability time increases from 10^5 years at 32.5 AU to 10^9 years at 37 AU.

As mentioned in Section 2.2, the three bodies in the inner Kuiper belt are all in mean motion resonance with Neptune. Conversely, 1992QB1 and 1993FW, which have $a > 43$ AU, cannot be associated permanently with any mean motion or secular resonance. The results of a 500-Myr numerical integration of the latter two bodies are plotted in Figs. 15 and 16.

The evolution of 1992QB1 seems to be quite regular. The semimajor axis oscillates between 43.6 and 44.3 AU. The eccentricity is modulated with a period of about 70 Myr. Such a modulation is associated with the slow circulation of the critical angle of the secondary secular resonance $\nu_8 + \nu_{18}$, with the maxima corresponding to $\varpi + \Omega - \varpi_N - \Omega_N = 0°$ and the minima corresponding to 180°. The inclination also has a very regular evolution and the long period modulation associated with the $\nu_8 + \nu_{18}$ term is also easily seen.

Starting with the initial conditions in Table I, the evolution of 1993FW is, by contrast, strongly irregular, especially for the behavior of the eccentricity and of the inclination.

The main reason for such irregularity seems to be the proximity of the 4/7 resonance with Neptune. From the picture of the evolution of the critical angle σ of the 4/7 resonance (Fig. 16), the object is temporarily captured in libration. At the same time, the argument of perihelion librates around 90°, indicating the existence of the Kozai resonance inside the 4/7 commensurability. As usual, the Kozai resonance couples the evolution of the eccentricity and of the inclination: the inclination decreases in correspondence with the eccentricity peaks.

Moreover, the critical angle of the $\nu_8 + \nu_{18}$ resonance also shows transitions from slow circulation to libration between 100 and 200 Myr, when the object comes out of
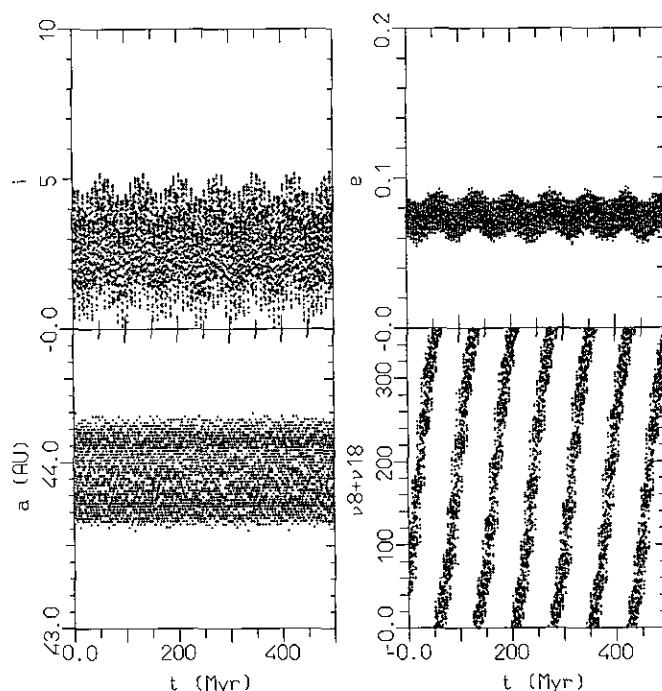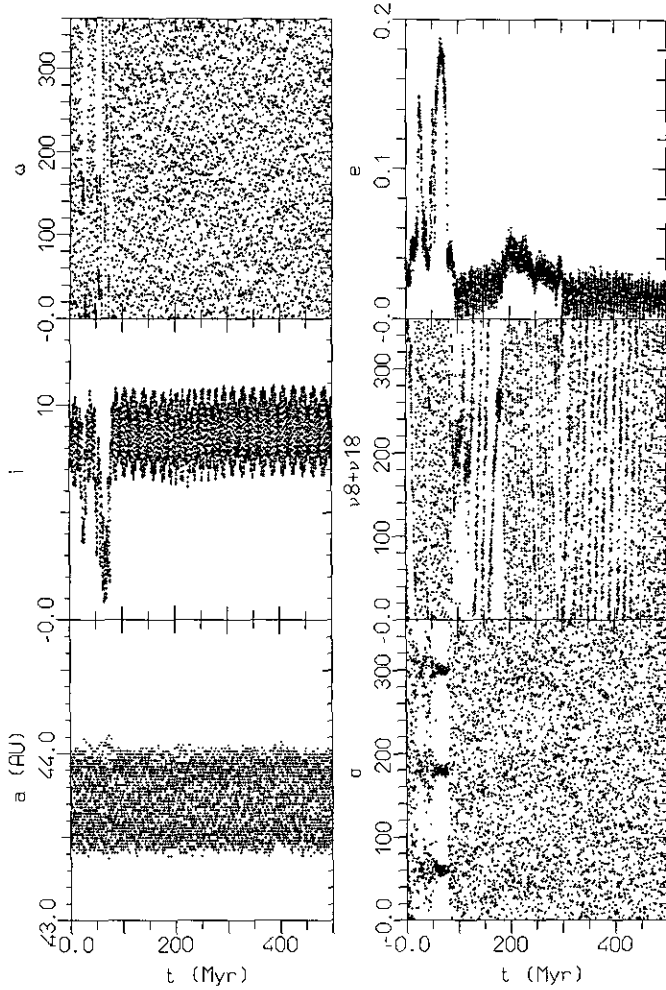

FIG. 15. The time evolution over 500 Myr of the heliocentric orbital elements of 1992QB1. Initial conditions are taken from MPC22594. Note the long periodic oscillation of e and i in phase with the circulation of $\nu_8 + \nu_{18} \equiv \varpi + \Omega - \varpi_N - \Omega_N$. See text for comments.

the 4/7 resonance. Between 200 and 300 Myr there is a change of behavior in the eccentricity, which is possibly due to temporary librations in the 4/7 resonance; the distribution of dots in the evolution of σ is somewhat more dense around the stable values of libration at 60°, 180° and 300°. From 300 Myr onward, the evolution of the orbit is quite regular.

From these considerations we can conclude that:

(1) 1993FW is very close and even temporarily inside the secondary secular resonance $\nu_8 + \nu_{18}$.

(2) The object is very close and temporarily inside the 4/7 mean motion resonance with Neptune, where the Kozai resonance is also found.

(3) The cause of irregularity may be the interaction among the secondary secular resonance, the mean motion resonance, and the Kozai resonance.

Finally, the eccentricity never exceeds 0.2, so that the object never comes close to Neptune, at least during the integration timespan, as can be noted from the stable evolution of the semimajor axis. Moreover, if our interpretation of the origin of the chaotic motion is correct, we should expect to find a very thin and localized chaotic layer, so that future improved determinations of 1993FW's orbit can put the object in a regular region. Indeed, in the preprint of Duncan *et al.* (1995) the assumed elements of 1993FW are

FIG. 16. The time evolution over 500 Myr of the heliocentric orbital elements of 1993FW. Initial conditions are taken from MPC23240. Here $\nu_8 + \nu_{18}$ denotes $\varpi + \Omega - \varpi_N - \Omega_N$ and σ is the critical angle of the 4/7 mean motion resonance with Neptune, i.e., $(-4\lambda_N + 7\lambda - 3\varpi)/3$. See text for comments.

slightly different and the body is found to be stable over 1 Gyr.

5. ANALYTICAL TOOLS FOR THE INVESTIGATION OF THE KUIPER BELT

This section is devoted to outlining the theoretical approach followed for the exploration of the dynamics and, in particular, for obtaining Figs. 1, 3, 5, 10, 12, and 17. All the tools used here have been developed and used for the study of the dynamics in the asteroid belt; further details can be found in Morbidelli and Moons (1993) and Moons and Morbidelli (1995) concerning mean motion resonances and in Morbidelli (1993) concerning secular resonances.

Our study in this paper is rough, and we introduce several simplifications and assumptions: the aim of this work

is to outline only the basic features of the dynamics in the Kuiper belt, without entering into complicated details. A more technical work will follow.

The starting Hamiltonian is that of a massless body perturbed by four planets on given orbits, i.e.,

$$\mathcal{H} = -\frac{1}{2a} - \sum_{j=1,4} \mu_j \left(\frac{1}{|\mathbf{r} - \mathbf{r}_j|} - \frac{\mathbf{r} \cdot \mathbf{r}_j}{r_j^3} \right), \qquad (1)$$

where $\mathbf{r}$ is the position of the massless body and $\mathbf{r}_j$ is the position of the jth perturbative planet with mass μ_j; the mass of the Sun and the gravitational constant are taken as unity.

The Hamiltonian (1) is divided in several parts, i.e.,

$$\mathcal{H} = \mathcal{H} + \mu\mathcal{H}_0 + \mu\mathcal{H}_0^i + \mu e'\mathcal{H}_1^e + \mu i'\mathcal{H}_1^i + O(e', i')^2, \qquad (2)$$

with μ denoting generically the mass of the perturbing planets. $\mathcal{H}$ is the Keplerian part $-\frac{1}{2}a$; $\mathcal{H} + \mu\mathcal{H}_0$ is the Hamiltonian of the planar circular restricted problem, where the planets are assumed to be on coplanar circular orbits and the inclination of the small body is neglected; $\mathcal{H}_0^i$ contains all the terms depending on the inclination of the massless body in the circular restricted problem; $\mathcal{H}_1^e$ is the part which is linear in the planetary eccentricities, denoted here generically by e'; $\mathcal{H}_1^i$ is the part which is linear in the planetary inclinations i'; $O(e', i')^2$ contains all the terms which are at least quadratic in the planetary eccentricities and/or inclinations and which are neglected in this theory. We stress that we do not use any expansion in the eccentricity and inclination of the small body, so that the quality of the results do not degrade with increasing e and i.

The Hamiltonian (2) is the basis of our theoretical investigation.

5.1. Mean Motion Resonances

The Hamiltonian (2) is time dependent through the mean longitudes λ_j of the planets; then the phase space is extended, introducing new actions Λ_j conjugate to λ_j.

Assuming the system to be close to a $(p + q)/p$ mean motion resonance with the j_*th planet, we introduce the canonical variables

$$\sigma = \frac{p+q}{q}\lambda_{j_*} - \frac{p}{q}\lambda - \varpi, \qquad S = L - G,$$

$$\sigma_z = \frac{p+q}{q}\lambda_{j_*} - \frac{p}{q}\lambda - \Omega, \qquad S_z = G - H,$$

$$-\nu = \frac{p+q}{q}\lambda_{j_*} - \frac{p}{q}\lambda, \qquad N = \frac{p+q}{p}L - H, \qquad (3)$$

$$\lambda_{j_*}, \qquad \Lambda'_{j_*} = \Lambda_{j_*} + \frac{p+q}{p}L,$$

$$\lambda_j, \qquad \Lambda_j,$$

where $L = \sqrt{a}$, $G = L\sqrt{1 - e^2}$, and $H = G \cos i$ are the actions conjugate to the mean anomaly l, the argument of perihelion ω and the longitude of the node Ω; the mean longitude $\lambda = l + \Omega + \omega \equiv l + \varpi$, where ϖ denotes the longitude of perihelion.

The Hamiltonian considered in a first step is that of the planar circular problem, i.e.,

$$\mathcal{H}^{res} = \sum_{j=1,4} n_j \Lambda_j + \mathcal{H} + \mu \mathcal{H}_0, \tag{4}$$

n_j denoting the mean motion of the jth planet. We stress that no expansion in σ is used for the calculation of the Hamiltonian in (4).

Furthermore, the Hamiltonian is averaged with respect to the fast angles λ_j and λ_{j*}; the resulting Hamiltonian is integrable, since it depends only on the angle σ. Indeed, the Hamiltonian is independent of ν since it does not depend, by construction, on the planetary eccentricities, so that it is rotationally invariant and reads

$$\mathcal{H}^{res} = \mathcal{H}^{res}(\sigma, S, N - S_z). \tag{5}$$

The study of this Hamiltonian is then a simple matter. On each surface $N - S_z = $ constant the dynamics is represented by the level curves of the Hamiltonian in a (σ, S) polar diagram. This can be simply converted into a $(e \cos \sigma, e \sin \sigma)$ diagram as in Figs. 10 and 17. The value of the constant $N - S_z = \sqrt{a}((p + q)/p - \sqrt{1 - e^2})$ associates a value of a to each value of e.

The width of the resonance is defined in the following way. From the unstable equilibrium point (at $\sigma = 0$ in Figs. 10 and 17a) stem the two separatrices of the resonance problem. The orbits between the two separatrices have a librating σ; these are the properly resonant orbits. Along the σ-libration the eccentricity changes and the maximal amplitude of this change corresponds to the intersection of the separatrices with the axis $\sigma = \sigma_{stab}$, σ_{stab} being the value of σ at the stable equilibrium points. With this computation made for each value of $N - S_z$, one gets the V-shaped limits of the resonant zones, as shown in Fig. 1, up to the planet-crossing limit.

For order-one resonances, decreasing $N - S_z$, the unstable equilibrium point disappears before reaching $e = 0$, so that the separatrices are no longer defined (see Henrard and Lemaitre 1983); this is the reason the V-shaped limits of the mean motion resonance of order-one in Fig. 1 are not defined all the way down to $e = 0$.

On a surface $N - S_z = $ constant which is above the planet crossing limit, the resonant phase space changes as in Fig. 17b. The collision with the planet is a singularity for the averaged Hamiltonian. However, orbits with librating σ with sufficiently small amplitude never approach the collisional region, so that they are phase-protected. This
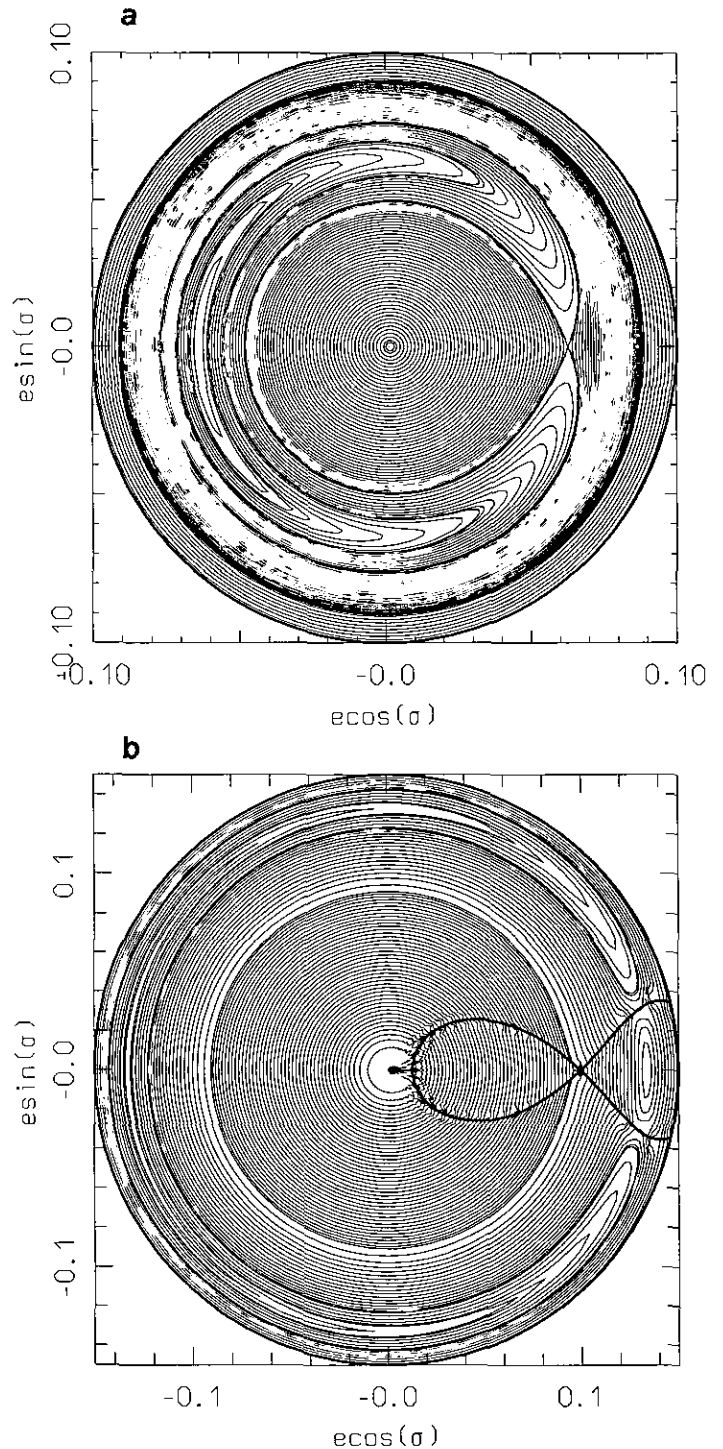
FIG. 17. (a) The phase space of the 5/6 resonance in a case where collision with Neptune cannot occur, $N - S_z = -0.96$. (b) The same, but in a case where collision with Neptune can occur, $N - S_z = -0.92$, the bold line denoting collision (the semimajor axis measured in AU). Librating resonant orbits are protected from collision. The width of the resonance is computed with respect to the largest banana-shaped librating orbit. Here σ is $-5\lambda_N + 6\lambda - \varpi$.

is not true, conversely, for orbits outside of the resonance, for which σ circulates. The width of the resonance above the planet-crossing limit is computed referring to the largest banana-like libration which avoids the planetary collision. Increasing $N - S_z$, i.e., the eccentricity, only orbits with smaller amplitude of σ-libration are protected. For this reason, in Fig. 1, the limits of the resonances, above the planet-crossing limit, shrink with increasing eccentricity. Moreover, the equilibrium point at $\sigma = 0$, which is unstable in Fig. 17a, becomes stable when the collisional singularity appears as in Fig. 17b. Orbits librating around this new stable equilibrium are also protected from planetary collisions. However, we will not refer to these orbits in the following analysis.

We come now to the investigation of the dynamics inside mean motion resonances.

In mean motion resonances of order one and at small eccentricity, the longitude of perihelion ϖ circulates fast with negative derivative, so that no secular resonances with the motion of the perihelia of the planets can occur. Indeed, the time derivative of ϖ is, in the variables (3), equal to $-\dot{\nu} - \dot{\sigma}$, i.e.,

$$\dot{\varpi} = -\frac{\partial \mathcal{H}^{\text{res}}}{\partial N} - \frac{\partial \mathcal{H}^{\text{res}}}{\partial S} = \frac{\partial \mathcal{H}^{\text{res}}}{\partial G} + \frac{\partial \mathcal{H}^{\text{res}}}{\partial H}.$$

We now show that $\partial \mathcal{H}^{\text{res}}/\partial G$ tends to $-\infty$ with $e \to 0$. Indeed, the first term of $\mathcal{H}_0$ in its expansion in powers of e is, as it is well known, $Ce \cos \sigma$, C being a negative coefficient. Therefore $\dot{\varpi}$ contains the term $C \cos \sigma(de/dG)$, where $C \cos \sigma$ is positive at the stable equilibrium $\sigma = 180°$. Now, $de/dG = -G/(eL^2)$, from which our claim directly follows.

In order to investigate the secular dynamics forced by the planetary eccentricities we proceed as follows. First, action angle variables (ψ, J) are introduced, such that (5) becomes independent of ψ, i.e., $\mathcal{H}^{\text{res}}(J, N - S_z)$. To be canonical, this transformation must be extended to σ_z and ν. The transformation on σ_z and ν is of the form $\sigma'_z = \sigma_z - \rho_{\sigma_z}(\psi)$, $\nu' = \nu - \rho_\nu(\psi)$, where ρ_{σ_z} and ρ_ν are periodic functions of ψ. By abuse of notation, in the following we still indicate as σ_z and ν the new angles σ'_z and ν'. The set of variables $(\psi, J, \sigma_z, S_z, \nu, N)$ must then be considered as canonical.

Then the term $e'\mathcal{H}_1^e$ proportional to the planetary eccentricities is taken into account and written in the new variables, which gives

$$\mathcal{H} = \mathcal{H}^{\text{res}}(J, N - S_z) + \mu e' \mathcal{H}_1^e(\psi, J, \nu + \varpi', N - S_z). \quad (6)$$

The term $\mathcal{H}_1^e$ depends on time through the planetary longitudes of perihelia, generically denoted here by ϖ'. For simplicity, in Fig. 3 only the perturbation given by

Neptune is taken into account and Neptune's perihelion is fixed (restricted elliptic three-body problem). This is a quite good approximation, since the perihelion of Neptune moves very slowly (0.67 arcsec/year). Then, assuming that there are no low-order resonances between the frequency of ψ and that of ν (i.e., no secondary resonances between the period of libration of σ and the period of circulation of ν), the Hamiltonian (6) is averaged with respect to ψ. The integrable Hamiltonian $\mathcal{H}(J, \nu + \varpi', N - S_z)$ describes the secular evolution of $N - S_z$ forced by the motion of $\nu + \varpi'$, for a given value of J, i.e, roughly speaking, for a given value of the amplitude of σ-libration. Since σ is librating around the stable equilibrium, $\nu + \varpi'$ is, in average with respect to ψ, equal to $\varpi' - \varpi - \sigma_{\text{stab}}$, where stab denotes the value of σ at the stable equilibrium point. Figure 3 is obtained in the limit $J \to 0$, and therefore concerns orbits on the stable equilibrium at $\sigma = 180°$.

In the spatial circular problem the Hamiltonian reads (Morbidelli and Moons, 1993)

$$\mathcal{H} = \sum_{j=1,4} n_j \Lambda_j + \mathcal{H} + \mu \mathcal{H}_0 + \mu \mathcal{H}_0^i.$$

With the new variables (3) it can be written as

$$\mathcal{H} = \mathcal{H}^{\text{res}}(\sigma, S, N - S_z) + \mu \mathcal{H}_0^i(\sigma, S, \sigma_z, S_z, N),$$

where $\mathcal{H}^{\text{res}}$ is the same as in (5).

As in the study above, the action angle variables (ψ, J) are introduced so that $\mathcal{H}^{\text{res}}$ depends only on the actions J and $N - S_z$. After the introduction of the new variables, $\mathcal{H}_0^i$ is averaged with respect to ψ and the Hamiltonian becomes integrable and reads

$$\mathcal{H}(J, \sigma_z, S_z, N) = \mathcal{H}^{\text{res}}(J, N - S_z) + \mu \mathcal{H}_0^i(J, \sigma_z, S_z, N).$$

Figure 5 describes the dynamics of such Hamiltonian in the case of the 2/3 resonance with Neptune, and in the limit $J \to 0$. The perturbations of the four planets are taken into account. Since σ librates, σ_z is nothing but the argument of perihelion ω and the resonance in the variables (σ_z, S_z) is the Kozai resonance which concerns the libration of ω. We have studied this resonance for several values of N and $J \to 0$ and we have determined its width, i.e., the values S_z corresponding to the separatrices at $\omega = 90°$. The values of S_z and N are then converted to e and i.

Moreover, we have computed the frequency of the node Ω, which, in the variables above, is given by $-\partial \mathcal{H}/\partial N - \partial \mathcal{H}/\partial S_z = \partial \mathcal{H}/\partial H$. As this is a function of σ_z, outside of the Kozai resonance we have computed its average value. The comparison of the averaged frequency of Ω with the nodal secular frequencies of the planets gives the location of the secular resonances. Their effects on the inclination of the small body could be observed only taking into ac-

count the $i'\mathcal{H}_1^i$ term. In the present work, however, we limit ourselves only to the determination of the location of secular resonances inside mean motion commensurabilities. In the 2/3 commensurability we have found only the existence of the ν_{18} resonance with the frequency s_8 of Neptune's node.

5.2. Secular Resonances

For the investigation of the dynamics in secular resonances outside mean motion commensurabilities, the set of variables (3) is let down and the usual actions L, $P = L - G$, and $Q = G - H$ conjugate to λ, $-\varpi$ and $-\Omega$ are used.

Since the fast angles λ and λ_j are non-resonant, the Hamiltonian (2) is averaged over all the mean longitudes. If the terms depending on the planetary eccentricities and inclinations are neglected, the averaged Hamiltonian

$$\mathcal{H}^{\mathrm{Koz}} = \mu\mathcal{H}_0 + \mu\mathcal{H}_0^i \qquad (7)$$

is integrable, since it depends only on the argument of perihelion ω of the small body, due to its rotational invariance. This Hamiltonian has been first studied by Kozai (1962). Recently, Thomas and Morbidelli (1995) extended Kozai's investigation to the Kuiper belt case, and found that the Kozai resonance can affect the motion of long-period comets but not the one of Kuiper belt objects on quasi-circular orbits.

In order to study the effects of order-one secular resonances with the precession motion of planetary orbits, Kozai's Hamiltonian (7) is extended, taking into account the terms $e'\mathcal{H}_1^e$ and $i'\mathcal{H}_1^i$. This introduces new time dependencies in the problem, since the planetary orbits are assumed to change with time with fundamental frequencies g_5, g_6, g_7, and g_8 for the perihelia, and s_6, s_7, and s_8 for the nodes. Therefore, we extend the phase-space of the problem, introducing new actions G_5, G_6, G_7, and G_8 conjugate to $\varpi_5' = g_5 t + \alpha_5^0$, $\varpi_6' = g_6 t + \alpha_6^0$, $\varpi_7' = g_7 t + \alpha_7^0$, and $\varpi_8' = g_8 t + \alpha_8^0$, and new actions S_6, S_7, and S_8 conjugate to $\Omega_6' = s_6 t + \beta_6^0$, $\Omega_7' = s_7 t + \beta_7^0$, and $\Omega_8' = s_8 t + \beta_8^0$. Here α_i^0 and β_i^0 are the initial phases. The values of the initial phases and of the frequencies can be found in Nobili et al. (1989).

With these settings, the Hamiltonian reads

$$\mathcal{H}^{\mathrm{sec}} = g_5 G_5 + g_6 G_6 + g_7 G_7 + g_8 G_8 + s_6 S_6 + s_7 S_7 + s_8 S_8$$
$$+ \mathcal{H}^{\mathrm{Koz}}(\omega) + \mu e'\mathcal{H}_1^e(\omega, \varpi, \varpi_5', \varpi_6', \varpi_7', \varpi_8')$$
$$+ \mu i'\mathcal{H}_1^i(\omega, \Omega, \Omega_6', \Omega_7', \Omega_8'), \qquad (8)$$

where the action variables have been omitted, for simplicity.

First, the Hamiltonian is averaged with respect to ω, since the Kozai resonance is far away in the case of the Kuiper belt. The averaged Kozai Hamiltonian $\mathcal{H}^{\mathrm{Koz}}$ depends now only on the actions P and Q and therefore has two constant frequencies $g \equiv -\partial\mathcal{H}^{\mathrm{Koz}}/\partial P$ and $s \equiv -\partial\mathcal{H}^{\mathrm{Koz}}/\partial Q$, which, following Williams (1969), are called the "proper frequencies" of the longitude of perihelion ϖ and of the node Ω.

To obtain Fig. 12, we now assume an isolated secular resonance, i.e., that there exists only one resonant relation between the planetary frequencies and the proper frequencies of the small body. In the case of the ν_8 resonance, for example, $g = g_8$; in the case of the ν_{18} resonance, conversely, $s = s_8$, etc.

We now average over the non-resonant planetary frequencies. As shown in Morbidelli and Henrard (1991), this provides the secular resonant models

$$\mathcal{H}^{\mathrm{sec.res}} = \mathcal{H}^{\mathrm{Koz}}(P, Q) + g_* G_* + \mu e'\mathcal{H}_1^e(P, Q, \varpi_*' - \varpi) \qquad (9)$$

for a secular resonance with the planetary perihelion frequency g_*, and

$$\mathcal{H}^{\mathrm{sec.res}} = \mathcal{H}^{\mathrm{Koz}}(P, Q) + s_* S_* + \mu i'\mathcal{H}_1^i(P, Q, \Omega_*' - \Omega) \qquad (10)$$

for a secular resonance with the planetary node frequency s_*. In the models above, instead of considering only the perturbation given by the planet for which the frequency g_* or s_* is dominating, the perturbations of all four planets are taken into account.

Both models are integrable, since they depend only on one angle, i.e., the critical angle of the involved secular resonance. Figure 12 refers to the ν_8 and ν_{18} resonances, the first computed for $Q \sim i^2 = 0$, the second for $P \sim e^2 = 0$. These models give a very accurate quantitative description of the real resonant dynamics as long as secular resonances are isolated (Morbidelli 1993). In the case of the Kuiper belt, conversely, secular resonances are not isolated, so that the models above are just qualitative. A two-resonance model could be introduced. For instance, in the case of the coexistence of the ν_8 and ν_{18}, this two-resonance model should be written

$$\mathcal{H}^{\mathrm{sec.res}} = \mathcal{H}^{\mathrm{Koz}}(P, Q) + s_8 S_8 + g_8 G_8 \qquad (11)$$
$$+ \mu i'\mathcal{H}_1^i(P, Q, \Omega_8' - \Omega) + \mu e'\mathcal{H}_1^e(P, Q, \varpi_8' - \varpi).$$

This model is strongly non-integrable, with possibly large chaotic regions. A detailed analysis on the chaotic dynamics in the presence of the overlap of secular resonances can be found in the work by Šidlichovský (1990).

6. CONCLUSIONS

From our analytical and numerical investigations of the dynamics in the Kuiper belt, we can draw the following conclusions:

• The mean motion resonances of order one with Neptune in the inner part of the Kuiper belt ($a < 39$ AU) are very stable, at least for small i, and provide a mechanism of phase-protection from close encounters with the planet.

• The 2/3 resonance with Neptune has a very complex dynamics; however, objects deeply inside the resonance, i.e., characterized by a small amplitude of libration, tend to have stable orbits. This is the case for 1993SB and 1993SC. Orbits with large amplitude of libration (as 1993RO, according to the initial conditions in MPEC-1994R06) have an irregular evolution due to the circulation/libration of their argument of perihelion ω, and could eventually escape the 2/3 resonance and encounter Neptune.

• Outer mean motion resonances (1/2, 2/5, 1/3, etc.) are quite regular and do not pump the eccentricity significantly, for moderate initial e and i.

• Secular resonances are present in the range $a \in [35, 36]$ AU and $a \in [40, 42]$ AU, at $i \sim 0$. The overlap of secular resonances gives rise to large scale chaos with a large increase in the eccentricity, which lead to Neptune-approaching orbits.

• Non-resonant orbits are not phase-protected from Neptune encounters and only orbits which are far enough from Neptune can be stable. The lower limit on a for stability depends therefore on the eccentricity. According to Levison and Duncan (1993), if the initial eccentricity is 0.1, then only orbits with $a > 42$ AU can survive 1 Gyr. The objects 1992QB1 and 1993FW have semimajor axes larger than 43 AU. The object 1992QB1 has a very regular orbit, while 1993FW has an irregular evolution due to the presence of a local small chaotic layer related to the 4/7 resonance and to a secondary secular resonance. In our numerical integrations, however, the eccentricity of this last object does not increase enough to approach Neptune at a dangerous distance.

From these conclusions we can now speculate on the structure of the distribution of bodies in the Kuiper belt. We suspect the inner part of the Kuiper belt to be the symmetric image of the outer part of the asteroid belt. In the inner part the Kuiper belt should be depleted, apart from the mean motion resonant regions which should be occupied by several members. Moreover, the recent theory by Malhotra (1995a) predicts that many bodies should have been captured into mean motion resonances due to the resonance sweeping caused by a slow change in Neptune's orbit. According to our results, most of these bodies, once captured, would have a stable evolution. We recall that the outer asteroid belt is completely depleted apart from

the Hilda and the Thule groups which are in the 3/2 and 4/3 resonances with Jupiter, respectively.

Beyond 42 AU, the Kuiper belt should carry a uniform distribution of objects. In contrast to the asteroid belt, the Kuiper belt should not have the equivalent of "Kirkwood gaps," since resonant effects are not strong enough.

According to this picture, it is not astonishing that the distribution of the number of presently known objects with respect to the semimajor axis follows a sort of Maxwellian-like curve (Jewitt and Luu 1995). The distribution of observed bodies should follow the mass distribution of the original nebula, which is supposed to decrease as a power law with respect to the inverse of the semimajor axis. However, in the inner part of the belt only the fraction of volume occupied by mean motion resonances can host long-lived objects. This is the reason the distribution of Kuiper belt members decreases, as the orbit of Neptune is approached.

The origin of the Jupiter family of comets is still an open question in the light of our paper. Indeed, in the present work we locate the regions characterized either by strong instability or by relevant stability, but the existence of these regions does not give a direct answer to the problem of the origin of comets. The regions which are strongly unstable should be, by now, empty of primordial bodies. In addition, comets cannot come from the stable parts of the Kuiper belt.

The numerical works (Holman and Wisdom 1993, Duncan 1994, Duncan et al. 1995) show that there are orbits in the Kuiper belt characterized by a slow "diffusion," which come to encounter Neptune only after some billion of years. These orbits seem to be initially located at the border of the regular regions (for example, they are large-amplitude librators in mean motion resonances), so that diffusion forces them to dive into the strongly unstable regions, where encounters with Neptune are then possible in a short time. Experiments show that if the test particles have initially a uniform density over the Kuiper belt, then the number of particles encountering Neptune at time T decreases approximately as $1/T$.

At present, the analytic theories are not able to map these regions and to identify all the secondary resonances which are involved in these diffusive processes, in the specific case of the Kuiper belt. However, on the base of the theory of Hamiltonian systems we understand that, as a general fact, in the transition between the strongly chaotic regions and regular regions, one must have orbits which diffuse over all possible time scales. More precisely, going from the strongly chaotic regions into the regular regions, the diffusion speed should decrease as $\exp(-1/(x_0 - x))$, where x "measures" the distance from the strongly chaotic region and x_0 is some parameter (typically related to the distance from the strongly chaotic region of the first invariant torus; the formula is valid, of course, only for $x < x_0$).

Then, at time T, the "regular" region has been eroded up to a depth $x \sim x_0 - 1/\log(T)$ (the formula being an asymptotic result, valid only for $T \gg 1$). Assuming that the particles have uniform density with respect to x, and differentiating the formula above with respect to T one has that the number of particles which dive at time T in the strongly chaotic region must decrease as $1/T$, which is in agreement with what the numerical experiments in the Kuiper belt indicate. An analogous result has been obtained numerically by Simó et al. (1995) in the very different case of the Froeschlé map. These theoretical considerations will be extended in a further paper.

From the astronomical point of view, the fact that the number of particles that encounter Neptune at time T decreases as $1/T$ means that, provided the initial density is large enough, there should still be a significant number of primordial bodies coming from the Kuiper belt and encountering Neptune at the present epoch. Duncan *et al.* (1995) estimate to 10^{10} the number of primordial bodies of kilometric size, to explain the presently observed number of small inclination comets. The recent observations, using the HST, by Cochran *et al.* (1995) seem to indicate that such a large number of proto-comets should exist in the Kuiper belt.

On the other hand, if such a large number of bodies exist in the Kuiper belt, then collisional evolution is possible (Stern 1995b). So, a second possibility for the origin of comets is that fragments are directly injected from the regular regions into the strongly unstable regions during collisional events, analogously to the mechanism that generates meteorites from the asteroid belt. A recent computation by Davis and Farinella (private communication) indicates that the number of comets injected into the unstable regions by collisions is on the same order of magnitude as the number of primordial bodies which dive into the unstable regions due to the above-mentioned diffusion.

The situation, however, is very fluid, and further studies and observations are necessary.

From the analysis of the first five objects, the orbits of which have been determined, although with relevant approximation, we believe that the majority of Kuiper belt bodies, which are presently being discovered, are stable members of the belt over the age of the Solar System. Again, it is certainly too early to draw definite conclusions. In particular, the number of known objects is, up to now, too small, and the determination of their orbits is too poor. Our results underline the necessity of an increasing number of observations in order to improve the number of known objects. In particular, it is crucial to have astrometric campaigns to determine with accuracy their orbit.

ACKNOWLEDGMENTS

REFERENCES

BEAUGÉ, C. 1994. Asymmetric librations in exterior resonances. *Celest. Mech. Dynam. Astron.* **60**, 225–248.

COCHRAN, A. L., H. F. LEVISON, A. S. STERN, AND M. J. DUNCAN 1995. The discovery of Halley-sized Kuiper belt objects using HST. *Astrophys. J.*, in press.

DUNCAN, M. J. 1994. Orbital stability and the structure of the Solar System. In *Circumstellar dust disks and planet formation* (R. Ferlet and A. Vidal-Madjat, Eds.), pp. 245–256. Editions Frontière, yif-sur-Yvette (France).

DUNCAN, M. J., T. R. QUINN, AND S. TREMAINE 1987. The formation and extent of the Solar System comet cloud. *Astron. J.* **94**, 1330–1338.

DUNCAN, M. J., T. R. QUINN, AND S. TREMAINE 1988. The origin of short-period comets. *Astrophys. J.* **328**, L69–L73.

DUNCAN, M. J., H. F. LEVISON, AND S. M. BUDD 1995. The long-term stability of orbits in the Kuiper belt. *Astron. J.*, in press.

EDGEWORTH, K. E. 1949. The origin and evolution of the Solar System. *Mon. Not. R. Astron. Soc.* **109**, 600–609.

FERNÁNDEZ, J. A. 1980b. On the existence of a comet belt beyond Neptune. *Mon. Not. R. Astron. Soc.* **192**, 481–491.

FESTOU, M. C., H. RICKMAN, AND R. M. WEST, 1994. Comets. *Astron. Astrophys. Rev.* **4**, 363–583.

HENRARD, J., AND A. LEMAÎTRE, 1983. A second fundamental model for resonance. *Celest. Mech. Dynam. Astron.* **30**, 197–218.

HEPPENHEIMER, T. A. 1979. Reduction to proper elements for the entire Solar System. *Celest. Mech. Dynam. Astron.* **20**, 231–241.

HOLMAN, M. J., AND J. WISDOM, 1993. Stability of test particle orbits in the outer Solar System. *Astron. J.* **105**, 1987–1999.

JEWITT, D. C., AND J. X. LUU 1995. The Solar System beyond Neptune. *Astron. J.* **109**, 1987–2002.

KNEŽEVIĆ, Z., A. MILANI, P. FARINELLA, CH. FROESCHLÉ, AND C. FROESCHLÉ, 1991. Secular resonances from 2 to 50 AU. *Icarus* **93**, 316–330.

KOZAI, Y. 1962. Secular perturbations of asteroids with high inclination and eccentricity. *Astron. J.* **67**, 591–598.

KOZAI, Y. 1985. Secular perturbations of resonant asteroids. *Celest. Mech. Dynam. Astron.* **36**, 47–69.

KUIPER, G. P. 1951. On the origin of the Solar System. In *Astrophysics: A Topical Symposium* (J. A. Hynek, Ed.), pp. 357–424. McGraw–Hill, New York.

LEVISON, H. F., AND M. J. DUNCAN 1993. The gravitational sculpting of the Kuiper belt. *Astrophys. J.* **406**, L35–L38.

LEVISON, H. F. AND M. J. DUNCAN 1994. The long-term dynamical behavior of short period comets. *Icarus* **108**, 18–36.

LEVISON, H. F. AND A. S. STERN 1995. Possible origin and early dynamical evolution of the Pluto–Charon binary. *Icarus* **116**, 315–339.

MALHOTRA, R. 1995a. The origin of Pluto's orbit: Implications for the Solar System beyond Neptune. *Astron. J.* **110**, 420–429.

MALHOTRA, R. 1995b. The phase space structure near Neptune resonances in the Kuiper belt. *Astron. J.*, in press.

MESSAGE, J. 1958. The search for asymmetric periodic orbits in the restricted problem of three bodies. *Astron. J.* **63**, 443–448.

MESSAGE, J. 1959. Some periodic orbits in the restricted problem of three bodies and their stabilities. *Astron. J.* **64**, 226–236.

Moons, M., and A. Morbidelli 1995. Secular resonances in mean motion commensurabilities: The 4/1, 3/1, 5/2, and 7/3 cases. *Icarus* **114**, 33–50.

Morbidelli, A. 1993. Asteroid secular resonant proper elements. *Icarus* **105**, 48–66.

Morbidelli, A. and J. Henrard 1991a. Secular resonances in the asteroid belt: Theoretical perturbation approach and the problem of their location. *Celest. Mech. Dynam. Astron.* **51**, 169–197.

Morbidelli, A., and M. Moons 1993. Secular resonances in mean motion commensurabilities: The 2/1 and 3/2 cases. *Icarus* **102**, 316–332.

Nacozy, P. E., and R. E. Diehl 1974. On the long-term motion of Pluto. *Celest. Mech. Dynam. Astron* **8**, 445–454.

Nacozy, P. E., and R. E. Diehl 1978. A semianalytical theory for the long-term motion of Pluto. *Astron. J.* **83**, 522–530.

Nobili, A., A. Milani, and M. Carpino 1989. Fundamental frequencies and small divisors in the orbit of the outer planets. *Astron. Astrophys.* **210**, 313–336.

Quinn, T. R., S. Tremaine, and M. J. Duncan 1990. Planetary perturbations and the origin of short-period comets. *Astrophys. J.* **355**, 667–679.

Schubart, J. 1964. Long-period effects in nearly commensurable cases of the restricted three body problem. *Smithson. Astrophys. Obs. Spec. Report* **149**.

Šidlichovský, M. 1990. The existence of a chaotic region due to the overlap of secular resonances ν_5 and ν_6. *Celest. Mech. Dynam. Astron.* **49**, 177–196.

Simó, C., M. Gómez, A. Jorba, and J. Masdemont 1995. The bicircular model near the triangular libration points of the restricted three body problem. In *From Newton to Chaos: Modern Techniques for Understanding and Coping with Chaos in N-Body Dynamical System* (A. E. Roy and B. A. Steves, Eds.), pp. 343–370. Plenum, London.

Stern, A. S. 1995a. The development and status of the Kuiper disk. *Completing the Inventory of the Solar System* (T. Bowell, Ed.). ASP, San Francisco.

Stern, A. S. 1995b. Collisional time scales in the Kuiper disk and their implications. *Astron. J.* **110**, 856–868.

Thomas, F., and A. Morbidelli 1995. The Kozai resonance in the outer Solar System and the dynamics of long-period comets. *Celest. Mech. Dynam. Astron.*, submitted.

Torbett, M. V., and R. Smoluchowski 1990. Chaotic motion in a primordial comet disk beyond Neptune and comet influx to the Solar System. *Nature* **345**, 49–51.

Williams, J. G. 1969. Secular resonances in the Solar System. Ph.D. dissertation, University of California, Los Angeles.

Williams, J. G., and G. S. Benson 1971. Resonances in the Neptune–Pluto system. *Astron. J.* **76**, 167–177.

Wisdom, J. 1985. A perturbative treatment of motion near the 3/1 commensurability. *Icarus* **63**, 272–289.

Wisdom, J., and M. J. Holman 1991. Simplectic maps for the *N*-body problem. *Astron. J.* **102**, 1528–1538.

Zheng, J. Q., M. J. Valtonen, S. Mikkola, M. Korpi, and H. Rickman 1995. Orbits of short period comets captured from the Oort cloud. In *Worlds in Interaction: Small Bodies and Planets of the Solar System.* (H. Rickman and M. J. Valtonen, Eds.), pp. 45–50. Kluwer, Dordrecht.